CHALMERS

Compensation of the displacement of a loudspeaker's diaphragm caused by an adjacent loudspeaker

OSCAR ALBINSSON

Department of Signals and Systems
Chalmers University of Technology
Göteborg, Sweden, 2009

EX095/2009

Preface

This master thesis work was done at the company Lab.gruppen for Chalmers University of Technology. The author follows the programme “Integrated Electronic Systems Design”, where this thesis was done in collaboration with the department of Signals and Systems, with Mats Viberg as examiner.

The work was carried out in a total of 20 weeks in the spring, summer and autumn of 2009. This project is referred to as X27 – Loudspeaker Compensation at Lab.gruppen, where the instructor was Klas Dalbjörn.

Artwork for the loudspeaker on the front page is done by Alexander Foss (foss1984@gmail.com, alexanderfoss.deviantart.com/gallery/).

The author would like to thank everyone that has made this master thesis work possible, you know who you are. Questions, opinions and such can be sent by mail to oscar.albinsson@gmail.com or oscara@student.chalmers.se.

X27 – Loudspeaker Compensation

Abstract

In two-way loudspeaker systems the sound pressure from the low frequency woofer will affect the position of the high frequency tweeters diaphragm. Two solutions for reducing the movement of the diaphragm are presented, in which the induced current is cancelled by a current with opposite phase. Both solutions rely on a filter that mixes in a cancellation voltage at the tweeter, where the input signals are the applied voltage at the woofer and the resulting induced current. A static filter has been implemented based on sweep measurements, and a suggestion of an adaptive filter solution based on the least mean squares (LMS) algorithm is also presented.

It has been proven that the acoustic coupling generates modulation distortion components, and that these can be reduced by applying a signal to compensate for the undesirable movement of the diaphragm. An analysis of the audibility of these components is done by utilizing equal loudness contours and masking curves. The results show that there are audible components in the lower frequency region. An ABX listening test was done to verify the audibility, but none of the subjects could distinguish a compensated system from a non-compensated. It is assumed that the results of the listening tests are caused by masking from the frequency content of the woofer.

History

Owner[1]: Oscar Albinsson

Approval group[2]: KLDAL, FRKIH, HEWIK

Rev.	Author	Review / APRD	Date	Comment
1B	OSALB			

Rev.	Revision number (1A, 1B, …, 2A, 2B, ….)
Author	Author's name or initials (the person responsible for creating the revision)
Review / APRD	Reviewer / Approvers initials (five letters)
Date	Date of review / approval
Comment	A short comment about the new revision (used as a change log)

[1] Person responsible for managing the document (assuring that it is reviewed, updated & approved)

[2] Persons(s) responsible for formally approving a document (changing from 'DRFT' to 'APRD')

Index

Figures

Terminology & Acronyms

ADC	Analog-to-Digital Converter
AMD	Amplitude Modulation Distortion
DAC	Digital-to-Analog Converter
DSP	Digital Signal Processor
DUT	Device Under Test
FMD	Frequency Modulation Distortion
HF	High Frequency (Speaker)
IMD	Intermodulation Distortion
LF	Low Frequency (Speaker)
LSB	Least Significant Bit
MLS	Maximum Length Sequence
MF	Middle Frequency (Speaker)
SNDR	Signal-to-Noise and Distortion Ratio
SNR	Signal-to-Noise Ratio
S/PDIF	Sony/Philips Digital Interconnect Format
SPL	Sound Pressure Level

1 INTRODUCTION

This master thesis work was done at the company Lab.gruppen for Chalmers University of Technology. The author follows the programme "Integrated Electronic Systems Design", where this thesis was done in collaboration with the department of Signals and Systems. The work was carried out in a total of 20 weeks in the spring, summer and autumn of 2009. This project is referred to as X27 – Loudspeaker Compensation at Lab.gruppen.

The report begins with a description of the task and the complications the coupling causes along with a description of the experimental setup. A theory chapter follows, which explains the basics for understanding modulation distortion and its causes. The method used for compensating the diaphragm displacement is given in Chapter 3, along with a description of how the equalizers for the JBL SRX712M speaker cabinet were generated. Implementation of the system that was used for cancelling the current is described in Chapter 4. The verification of the compensation, distortion measurements and a description of the listening test is given account for in Chapter 5. Results and other subjects are discussed in Chapter 6, followed by conclusions in Chapter 7 and suggestions for future work in Chapter 8. A number of practical challenges that occurred are described in Appendix A.

1.1 Description of the task

A 2-way loudspeaker system usually contains a woofer (low frequency driver) and a horn loaded tweeter (high frequency driver), which radiate low and high audio frequencies respectively, where each loudspeaker is driven by separate amplifier channels. The acoustic coupling between the bands will affect the respective positions of the cones as a loudspeaker also acts as an electrodynamic microphone. It is anticipated that the displacement of the tweeter due to woofer coupling causes undesirable artifacts, whereas the effect on the woofer from the tweeter is negligible. A way to prevent this is to compensate for the displacement by mixing in a cancellation signal to the speaker. In Figure 1, a block diagram of this system is shown, where X_{LF} and X_{HF} are the signals intended for the woofer and tweeter respectively. These are amplified by a gain factor G resulting in the output voltages V_{LF} and V_{HF}. The magnitude and phase of the cancellation signal is determined by the filter H.

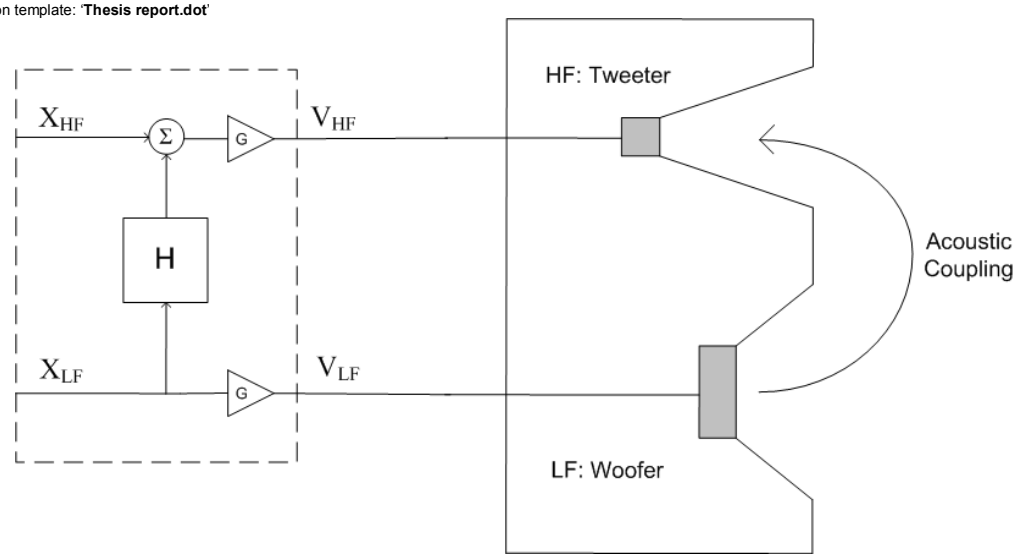

Figure 1: Block diagram of the compensation system where the cancellation signal is generated by the filter H

In order to know how the tweeter is affected by the woofer it is necessary to examine the speakers more closely. A simplified electro-mechanical model of the woofer is shown in Figure 2, where the electrical parameters of the speaker are the voltage u_{LF} [V], impedance Z_e [Ω] and current i_{LF} [A]. The current i_{LF} gives rise to a mechanical force on the diaphragm f_d [N] through the force field factor $B \cdot l$ [Tm], resulting in a velocity u_d [m/s] through the mobility Y_M [m/Ns]. The mechanical motion moves air by the force f_r [N] through the radiation mobility Y_{MR} [m/Ns], resulting in a sound pressure p [Pa] and a volume velocity U [m³/s] [1].

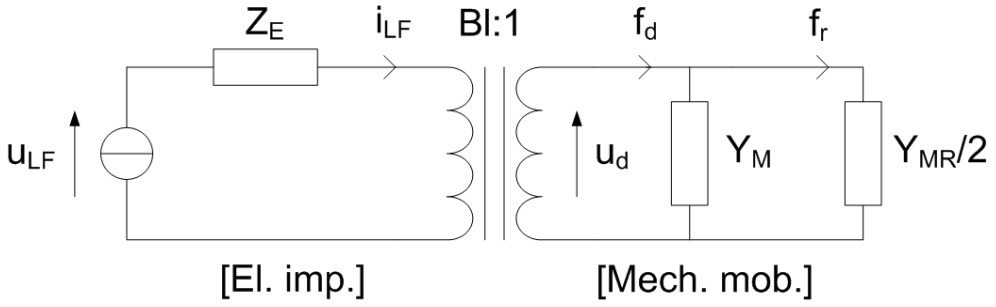

Figure 2: Electro-mechanical model of the woofer

It can be assumed that the tweeter acts as an electrodynamic microphone generating a current from the sound pressure of the woofer. A model for its acoustical-mechanical-electrical behavior is shown in Figure 3, where the sound pressure p along with the volume velocity U_d generates a mechanical motion through the diaphragm area S [m²]. This force f_d generates a diaphragm velocity u_d through the mechanical mobility Y_M. An electric current i_{HF} is generated by the force field factor $B \cdot l$, which gives rise to a voltage u_{HF} through the impedance Z_e [1].

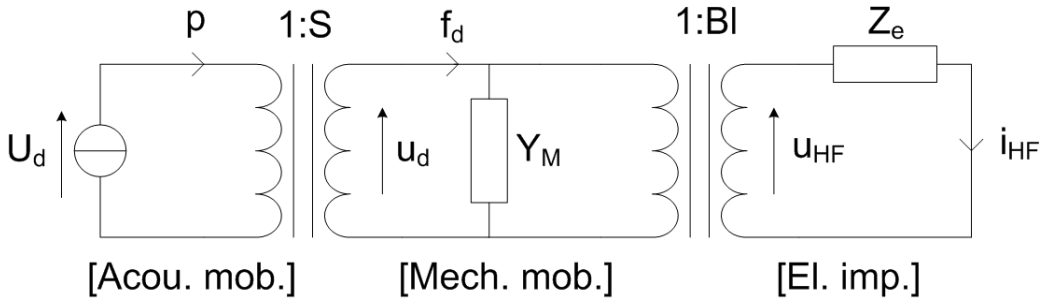

Figure 3: Acoustical-mechanical-electrical model of the tweeter

The purpose of the compensation is to disable the movement of the tweeter diaphragm caused by the woofer. This corresponds to a zero velocity u_d when no signal is applied on the HF. Most loudspeaker manufacturers do not give away the parameters required to calculate the components of the mechanical mobility and hence the velocity of the diaphragm. Recalling Figure 3, it can be seen that a zero velocity u_d implies that the induced current i_{HF} is zero as well. It is therefore sufficient to study the electric current through the tweeter. By measuring the applied voltage at the LF and the induced current of the HF it is possible to obtain a transfer function that describes the behavior of the coupling. This transfer function could be used to create a filter which generates a current with an opposite phase that cancels out the induced current. It is assumed that if the induced current is zero the velocity will be zero.

1.2 Background

Originally the coupling between different speakers was discovered when an algorithm for verifying the impedance of loudspeakers during use gave erroneous measurements. The impedance response measurements turned out to be affected by nearby drivers. It was also anticipated that the coupling might modulate the small-signal driver parameters of the horn, hence affecting the sound quality of the speaker. Therefore, it was decided that it had to be investigated further resulting in the current thesis project X27 – Loudspeaker Compensation.

1.3 Thesis Goals

The following goals were set in the beginning of the thesis.

- Find a way to determine how the parts of the system influence the diaphragm of the tweeter.
- Implement a system that compensates for this deviance
- Measure the difference from the previous implementation
- Make subjective evaluations to verify the improvement

It was decided that the methods described in this report are limited to two-way loudspeakers of the same type as the JBL SRX712M, although it might work on other kinds of loudspeakers as well.

1.4 Experimental setup

This chapter describes the devices that were used for measuring and verifying the compensation, namely; the loudspeaker: JBL SRX712M, the power amplifier: Lab.gruppen

PLM 10000Q, the sound card: MOTU 828mkII Firewire and the measurement microphone: Behringer ECM8000.

1.4.1 Loudspeaker: JBL SRX712M

The JBL SRX712M is a two-way stage monitor with the specifications given in Table 1.

Table 1: Specifications for the JBL SRX712M [9]

System Type:	12", two-way, bass-reflex, stage-monitor / utility
Frequency Range (-10 dB):	70 Hz – 20 kHz
Frequency Response (±3 dB):	83 Hz – 18 kHz
Coverage Pattern:	50° x 90° nominal (Monitor position)
Crossover Modes:	Bi-amp / passive, externally switchable
Crossover Frequency:	1.2 kHz
Power Rating (Continuous[1] / Program / Peak):	Passive: 800 W / 1600 W / 3200 W Bi-amp LF: 800 W / 1600 W / 3200 W Bi-amp HF: 75 W / 150 W / 300 W
Maximum SPL[2]:	131 dB SPL peak
System Sensitivity (1w @ 1m):	96 dB SPL (passive mode)
LF Driver:	1 x JBL 2262H 305 mm (12 in) Differential Drive woofer
HF Driver:	1 x JBL 2431H 75 mm (3 in) voice coil, neodymium compression driver
Nominal Impedance:	Passive: 8 ohms Bi-amp LF: 8 ohms Bi-amp HF: 8 ohms
Active Tunings:	dbx DriveRack, all models. Settings available at www.jblpro.com
Enclosure:	Symmetrical stage monitor, 15 mm, 11-ply birch plywood.
Suspension / Mounting:	Dual-angle (0° or -10°), 35 mm pole socket 2 x M10 fittings for optional SRX712M-YK yoke
Transport:	Integrated handle / input cup
Finish:	Black DuraFlex finish
Grille:	Powder coated, black, 16-gauge perforated steel with acoustical transparent charcoal foam backing. Removable JBL badge and punched JBL logo.
Input Connectors:	Neutrik® Speakon® NL-4 (x2), one on each end
Dimensions (H x W x D):	349 mm x 546 mm x 260 mm (13.75 in x 21.5 in x 10.25 in)
Net Weight:	15 kg (33 lb)
Optional Accessories:	SRX712M-CVR: Pull-over padded cover SRX712M-YK: Suspension / mounting yoke

1) IEC filtered noise with 6 dB crest factor

2) Calculated based on power rating and sensitivity

Impedance measurements done with the speaker model tool LoadEd developed by Lab.gruppen are shown in Figure 4 for the woofer and Figure 5 for the tweeter.

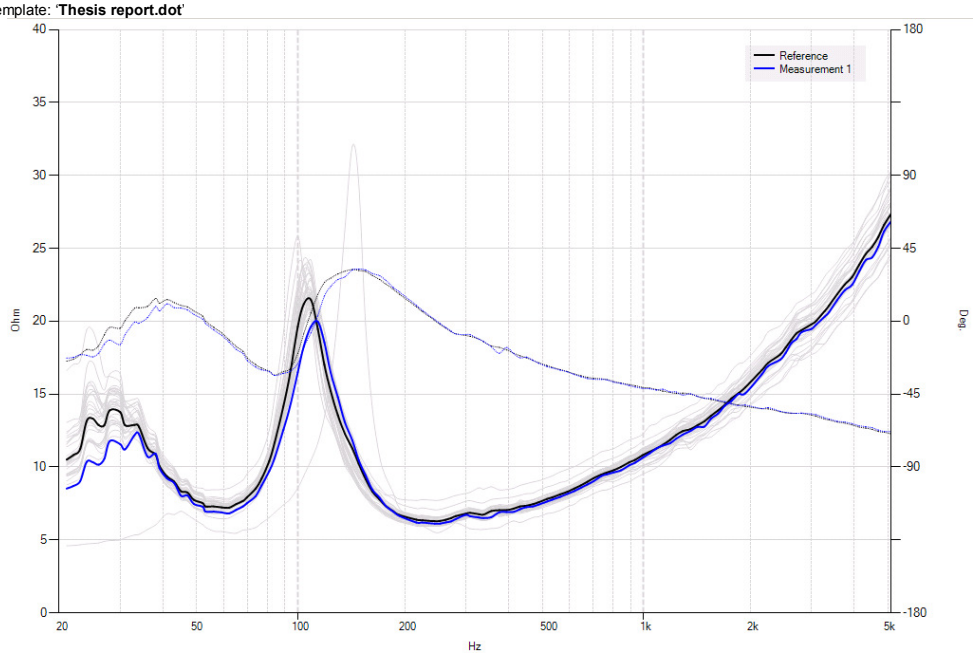

Figure 4: LoadEd impedance measurement of the woofer in the JBL SRX712M loudspeaker

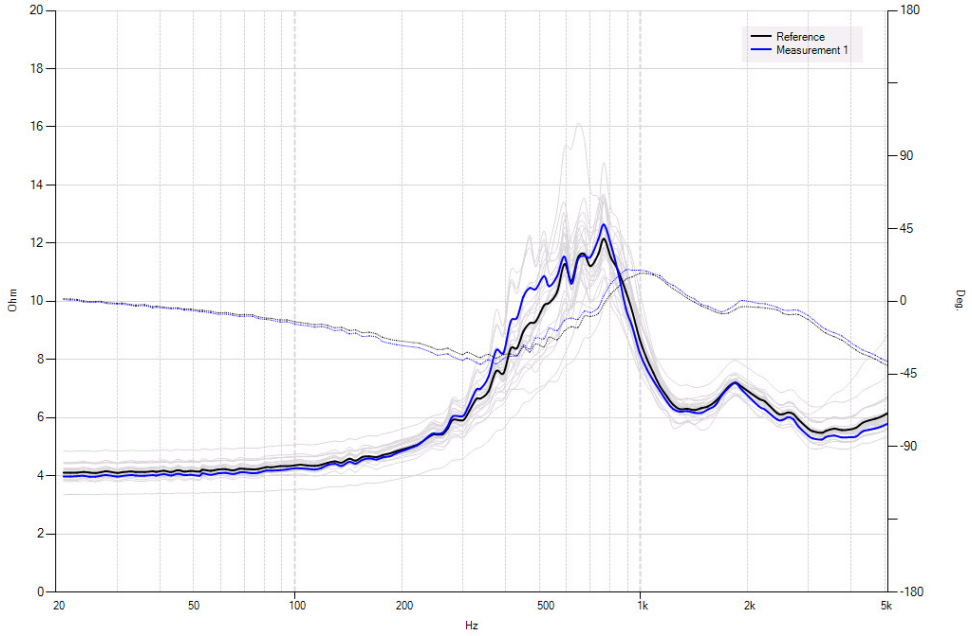

Figure 5: LoadEd impedance measurement of the tweeter in the JBL SRX712M loudspeaker

In Figure 4 and Figure 5 the blue lines are the result of the last measurement and the black lines are the mean value of all the previous measurements on the same type of loudspeaker. The shaded lines represent all the previous measurements of the same device. It can be seen in Figure 4 that the resonance frequency for the woofer is located around 120 Hz and that the deviance in the impedance is high around this point. The impedance of the tweeter in Figure 5 indicates a resonance frequency at around 650 Hz and that the variations are large in the proximity of this frequency.

1.4.2 Power amplifier: Lab.gruppen PLM10000Q

The PLM10000Q is a two input, four output power amplifier utilizing Class TD. It has an internal software environment called Lake Controller, in which the user can control parameters for equalization, limiting, delay, routing and other functions. Lake Controller is run on a computer and communicates with the PLM10000Q through an Ethernet connection. Digital audio can be transmitted and received through this connection with the Dante networking solution [10]. Some selected specifications of interest are given in Table 2.

Table 2: Selected specifications PLM10000Q [10]

Max. Output Power:	1300 W/channel @ 8 Ohms
Max. Peak output voltage per channel:	153 V
Max. Peak output current per channel:	49 A
Peak total output all channels driven:	10800 W
THD + N 20 Hz – 20 kHz for 1 W:	<0.05 %
Dynamic Range with digital inputs:	>116 dBA
Dynamic Range with analog inputs:	>114 dB
Amplifier gain:	22 – 44 dB, step size 0.1 dB
Internal sample rate:	96 kHz
Internal data path:	32 bit floating point

There are internal voltage and current probes in the amplifier, which are routed through the P20 WorkBench software. The data from the probes are distributed through the Dante virtual sound card and can be recorded with any recording software compatible with ASIO drivers. It is possible to record the data from two probes at the same time.

1.4.3 Sound card: MOTU 828mkII Firewire

The MOTU 828mkII is a firewire audio interface with 20 separate inputs and 22 outputs. There are S/PDIF connections for digital audio and analog connections which use a conversion at 96 kHz/24 bits. The maximum output voltage for the analog ¼" balanced TRS connections is 4 dBu. The sound card is compatible with ASIO drivers and has an internal DSP and mixer. There are also two built-in microphone pre-amps, each with a 48 V phantom power supply [12].

1.4.4 Measurement microphone: Behringer ECM8000

The Behringer ECM8000 is an electret condenser measurement microphone with a linear frequency response within ±1 dB from 15 Hz to 20 kHz and an omnidirectional directivity. It can be phantom powered from 15 V to 48 V, has an impedance of 600 Ω and sensitivity of -60 dB [11]. All measurements were done with a phantom power at 48 V.

2 Theory

This chapter gives some background theory about modulation distortion in loudspeaker and the factors that cause it. Both amplitude and modulation distortion are given account for as well as how audible the resulting components are in terms of equal loudness and masking.

2.1 Modulation Distortion

The first findings of modulation distortion in loudspeakers were made by Beers and Belar in 1943 [2]. At this point, most of the loudspeakers covered the entire audio frequency range. A full-range speaker of this kind will in higher degree be subject to both amplitude modulation distortion (AMD) and frequency modulation distortion (FMD) than a two-way loudspeaker.

Amplitude modulation distortion results from mixing two signals with different frequencies and applying them to a nonlinear device. Frequency modulation distortion arises due to the fact that loudspeaker cones have a mechanical motion, from which distortion components are generated by the Doppler effect [4]. These types of distortion are commonly known as intermodulation distortion (IMD) and a lot of research of this phenomenon has been done in the area of communication systems [3]. The frequency components that are generated by modulation distortion are not multiples of the fundamental tone, as with harmonic distortion. Instead, they appear as differences and sums of the two present frequencies and at higher orders of them. It should be noted that when amplitude modulation occurs, harmonic distortion components will also be present [6].

If the modulating frequency is located at f_0 and the higher modulated frequency at f_1,the resulting sideband distortion components will be located at the frequencies given in Equation (1), where p and n are positive integers [5].

$$\begin{aligned} & f_1 \pm f_0 \\ & f_1 \pm 2 \cdot f_0 \\ & \ldots \\ & p \cdot f_1 \pm n \cdot f_0 \end{aligned} \qquad (1)$$

It is primarily distortion components of the second order e.g. $p + n = 2$ that are relevant to consider in loudspeakers [5]. The amplitudes of these sidebands are dependent on both the FMD and AMD, which will be discussed further in Chapter 2.1.1 and 2.1.2 respectively.

Klipsch made a note on modulation distortion for two-way coaxial and spaced loudspeaker systems, where it was assumed that the predominant cause of modulation distortion for these was that the sound from the tweeter diffracts and is reflected by the woofer cone. It was also assumed that the tweeters displacement depending on the sound pressure from the woofer was a negligible cause of modulation distortion [18]. Experiments showed that the modulation distortion from a spaced system was hardly audible, but that from a coaxial speaker clearly audible. Further experiments on coaxial speakers by Suzuki and Shibata showed that the static displacement of the woofer affects the radiation efficiency of the tweeter, resulting in AMD. It was also shown that the FMD had a magnitude of the same size as the AMD, caused by the non-flat parts of the vibrating woofer [19]. These results indicate that there is a lower limit in how much the modulation distortion can be reduced, especially for coaxial speakers. These acoustical phenomena are independent upon the displacement of the tweeters diaphragm.

2.1.1 Frequency Modulation Distortion

As previously mentioned, frequency modulation distortion is caused by the Doppler effect. A classic example is that of an ambulance with its sirens on driving past an observer, who will

hear a change in pitch. The same thing happens if a loudspeaker moves with a modulation frequency f_0 and at the same time reproduces a frequency at f_1. Since the cone moves towards and away from the listener at a frequency f_0, the energy at the upper frequency f_1 will be subject to frequency modulation [6].

The equation that describes frequency modulation, which originally was given by Terman and later modified by Klipsch [4], is expressed in Equation (2) where; E is the amplitude at f_1; ω_0 and ω_1 are the angular velocities at f_0 and f_1 respectively; $\Delta\omega_1$ is the maximum deviation of the angular velocity ω_1.

$$e = E \cdot \sin\left[\omega_1 t + (\Delta\omega_1 / \omega_0) \cdot \sin(\omega_1 t)\right] \tag{2}$$

It is common practice to define the factor $\Delta\omega_1 / \omega_0$ as the modulation index m [6]. This index can be rewritten as in (3), where c is the speed of sound and $V = A_0\omega_0$ is the peak velocity of the cone,

$$m = \Delta\omega_1 / \omega_0 = \frac{(V/c)\omega_1}{\omega_0} = \frac{A_0\omega_0}{c} \cdot \frac{\omega_1}{\omega_0} = \frac{A_0}{c} \cdot \omega_1 \tag{3}$$

If (2) is expanded into its Bessel form with $E = 1$ and $m = \Delta\omega_1 / \omega_0$, the following relation is obtained

$$\begin{aligned} e = E \cdot \sin\left[\omega_1 t + m \cdot \sin(\omega_1 t)\right] = \\ = J_0 m \sin(\omega_1 t) \\ + J_1 m\left[\sin((\omega_1 + \omega_0)t) - \sin((\omega_1 - \omega_0)t)\right] \\ + J_2 m\left[\sin((\omega_1 + 2\omega_0)t) - \sin((\omega_1 - 2\omega_0)t)\right] \\ + ... \\ + J_n m\left[\sin((\omega_1 + n\omega_0)t) - \sin((\omega_1 - n\omega_0)t)\right] \end{aligned} \tag{4}$$

If the modulation index m is larger than 1, a high number of terms J_k of the Bessel function has to be included. In the audio frequency range the modulation depth is not as large as in radio frequency applications [5]. Hence, it is only necessary to include terms up to the second order; these are given by,

$$\begin{aligned} e_0 &= J_0 m \cong 1 \\ e_1 &= J_1 m \cong m/2 \\ e_2 &= J_2 m \cong m^2/8 \end{aligned} \tag{5}$$

An approximated speed of sound at $c = 340$ [m/s] results in,

$$\begin{aligned} e_0 &= 1 \\ e_1 &= 0.0091 A_0 f_1 \\ e_2 &= 6.8 \cdot 10^{-6} \cdot (A_0 f_1)^2 \end{aligned} \tag{6}$$

It is important to note that the magnitudes in (6) are given for each sideband. The total FMD amplitude would therefore with components up to e_2 correspond to $A_{FMD} = 2 \cdot e_1 + 2 \cdot e_2$.

2.1.2 Amplitude Modulation Distortion

Amplitude modulation distortion generates frequency components that are identical to those generated by FMD, as well as harmonic distortion. It is the nonlinearity of the device that

generates these components. Nonlinearities that are common in loudspeakers are given account for in Chapter 2.2. Consider a nonlinear transfer function as,

$$Y = a_1 X + a_2 X^2 + a_3 X^3 \tag{7}$$

A third order term would with an input signal $X = \sin(\omega_0 t) + \sin(\omega_1 t)$ give rise to the following additional frequency components [5];

$$\begin{aligned} a_3 X^3 &= a_3(\sin(\omega_0 t) + \sin(\omega_1 t))^3 = \\ &= a_3(\sin^3(\omega_0 t) + 3\sin^2(\omega_0 t)\sin(\omega_1 t) \\ &\quad + 3\sin(\omega_0 t)\sin^2(\omega_1 t) + \sin^3(\omega_1 t)) = \\ &= a_3(3/4\sin(\omega_0 t) - 1/4\sin(3\omega_0 t) \\ &\quad + 3/4\sin(\omega_1 t) - 1/4\sin(3\omega_1 t) \\ &\quad + 3/2\sin(\omega_0 t) + 3/2\sin(\omega_1 t) \\ &\quad - 3/2\sin(\omega_0 t + 2\omega_1 t) \\ &\quad - 3/2\sin(\omega_0 t - 2\omega_1 t) \\ &\quad - 3/2\sin(\omega_1 t + 2\omega_0 t) \\ &\quad - 3/2\sin(\omega_1 t - 2\omega_0 t)) \end{aligned} \tag{8}$$

The result in (8) is obtained by using the double-angle and product-to-sum trigonometric identities. A closer look at the four last terms reveals that sideband components are generated at $\omega_0 \pm 2\omega_1$ and $\omega_1 \pm 2\omega_0$. There are also 3rd order harmonics present which have no analogy in FMD. A second order nonlinearity will give rise to sideband components at $\omega_0 \pm \omega_1$ and $\omega_1 \pm \omega_0$. The amplitude of the AMD components is dependent on the amount of amplitude nonlinearity in the device. It is not possible to calculate coefficient a_1 in (7), but it can be measured [6]. A way to measure the amplitude modulation distortion has been given by Richard H. Small in 2003 [7].

2.1.3 Audibility of Modulation Distortion

The audibility of FMD and AMD is dependent on where the modulating signal f_0 and the carrier signal f_1 is located. Of importance is also the order of the sidebands that are produced and their magnitude. What type of excitation that is used does also affect the audibility, e.g. two tones, noise, music etc.

Psychoacoustic perception is of course individual, but some common sensations have been described by Mihelich [8]. At low modulating frequencies, below 15 Hz, the envelope of the carrier frequency can be heard resulting in a sensation called fluctuation strength which reminds of a tremolo effect.

At modulating frequencies between 15 Hz to 300 Hz, the amplitude variations of the carrier are no longer audible but instead, the carrier frequency sounds rough. A describing word of this sensation is roughness and can in most cases only be heard by experienced listeners.

When the modulation frequency is raised to the area around hundreds of Hz, the sideband frequencies are perceived as separable tones. The audibility of these tones is mainly dependent on two psychoacoustic phenomena called equal loudness and masking. Equal

loudness contours give the sound pressure level at which a tone at a certain frequency is perceived as equally loud as a tone at 1 kHz. This relation is not linearly related to the sound pressure level of this tone, resulting in different curves at different levels, which are defined by the ISO226 standard [13]. The equal loudness curve has been generated by a number of listening tests and has the unit Phon. Examples of equal loudness curves generated by the ISO226 standard for a 1 kHz tone at 30 dB_{SPL} and 80 dB_{SPL} are shown in Figure 6.

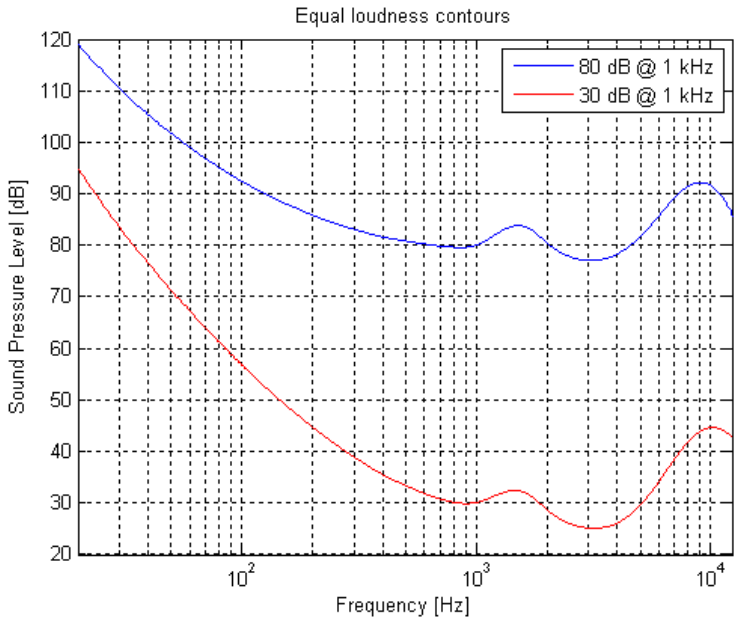

Figure 6: Equal Loudness Contours, which describe at which a tone at a certain frequency is perceived as equally loud as a tone at 1 kHz.

Masking occurs when the audibility of a sound is blocked when another sound is present. The sound that causes this impact is called the masker and the sound that is affected is called the maskee. This phenomenon is also nonlinear and has been measured by listening tests.
Figure 7 shows the minimum sound pressure level a maskee can be heard at in the presence of a masker at 1 kHz at different levels. The broken line shows the hearing threshold for the human ear.

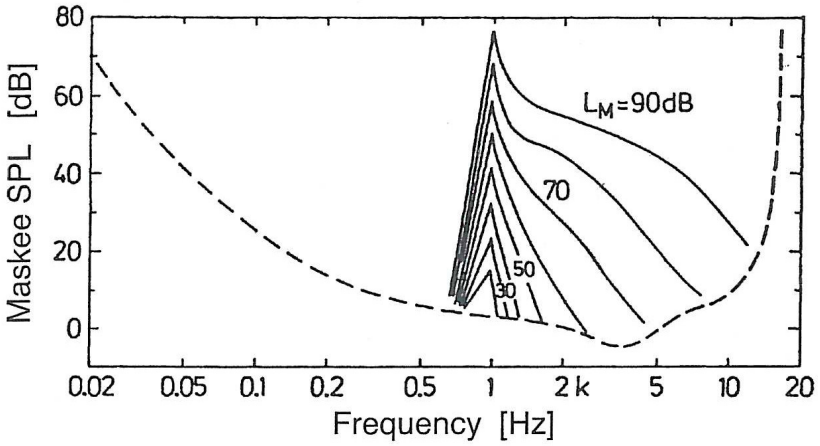

Figure 7: Sound pressure levels at which a masked tone can be heard in the presence of a masker at 1 kHz at different levels. (With kind permission of Springer Science + Business Media) [14].

As can been seen in Figure 7 the required sound pressure level of the maskee is higher for the frequencies above the masker.

2.2 Loudspeaker Nonlinearities

The force that is applied on a loudspeaker by an electric current is given in (9) where; F is the force [N], B is the magnetic flux density [T], l is the length of the wire around the voice coil [m] and i is the applied current [A] [13].

$$F = B \cdot l \cdot i \tag{9}$$

The main contributor to AMD is the force factor $B \cdot l$, which varies with the coil displacement. If the force factor is symmetric, odd order sideband components will be generated. An asymmetric system produces even order distortion components. In most loudspeakers the flux-field density B is an asymmetric nonlinear function [8]. Another significant nonlinear part is the coil, which has a self-inductance that varies with the displacement of the diaphragm. There are also a number of other nonlinear contributors that affects the AMD to a lesser degree, which have been described by Richard H Small [7].

A loudspeaker can also be considered as a mechanical device which is set into motion, as described in Chapter 1.1. The required force to set the diaphragm in motion is given in (10), where the voice coil's acceleration, velocity and displacement are given by a, v and x respectively. The mechanical mass, resistivity and compliance are given by M_M, R_M and C_M [13].

$$F = M_M \cdot a + R_M \cdot v + \frac{x}{C_M} \tag{10}$$

The mechanical compliance C_M is mainly determined by the air inside the loudspeaker and the compliance of the suspension. The stiffness of the suspension is non-linear and is thus also a source of amplitude modulation distortion. In some designs, it gives rise to almost the same amount of AMD as the force factor [7].

3 Method

This chapter describes the measurement setup as well as the methods for compensating the coupling between the speakers. Two different solutions for generating the compensation filter are given account for; a static version, where the filter is estimated by a single measurement and a solution based on an adaptive filter utilizing the LMS algorithm. A description of how the equalizers for the woofer and tweeter were generated is also included.

3.1 Measurement Setup

The setup used for measuring the signals of interest is shown in Figure 8, where a PC running the software Tracktion is connected to the power amplifier PLM10000Q through an Ethernet connection with the Dante virtual sound card. The device under test (DUT) is connected to the output of the power amplifier and two probes located inside the amplifier give the data from the measurement.

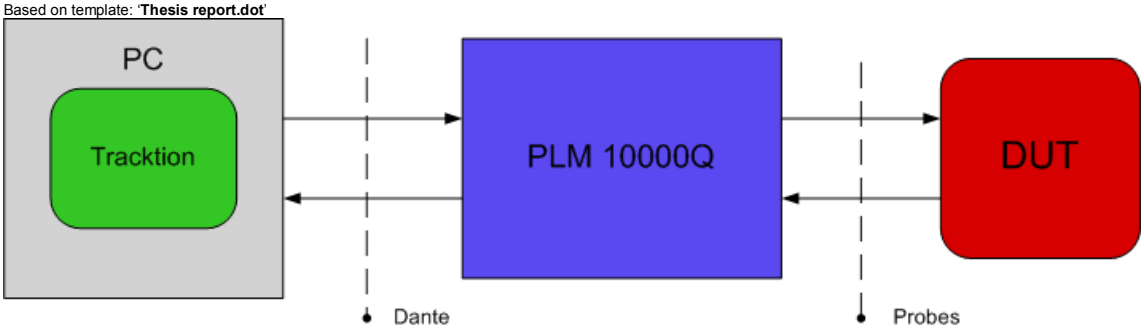

Figure 8: Measurement setup. Note that the probes actually are inside the PLM.

Tracktion is a recording software created by Mackie [20], which has support for recording and playback of multiple channels in full-duplex mode. The excitation signal was imported into this program as a wave-file. Dante was set up as a virtual sound card in the PC with a sampling frequency of 96 kHz and a resolution of 24 bits, using ASIO drivers. The setup in the power amplifier PLM 10000Q is described in Chapter 1.4.2 along with the probes.

3.2 Measurement Method

The signals that the user has direct control over at the power amplifier outputs are the applied voltages. Therefore, the woofer was excited with repeated logarithmic sweeps while the resulting voltage across it along with the current at the tweeter was measured. A more intuitive solution would be to measure the voltage at the tweeter but this was not possible because of the hardware solution at the output probes.

Logarithmic sweeps were used as excitation signals since the measurement becomes less sensitive to time variance and distortion than if noise excitations would have been used. A higher signal-to-noise ratio than in MLS (Maximum Length Sequence) measurements can also be obtained [16]. The magnitude spectrum of a logarithmic sweep drops by 3 dB/octave because the time period each frequency is excited decreases as the frequency increases, hence lowering the energy in that band. Since it is the transfer function which is the point of interest, this anomaly is cancelled out by the following mathematical operations. The magnitude drop could however cause problems if measurements are done close to the noise floor. One would suggest that a linear sweep could be used in that case, but it is generally not a good idea since the risk of damaging the loudspeaker increases.

A logarithmic sweep from 30 Hz to 3 kHz was created in MATLAB, where the frequency range was chosen to be a bit wider than the band of interest so that the recorded signals could be windowed, as described in Chapter 3.3. In order to avoid damaging the speaker and to reduce the calculation time further on, the length of the sweep was set to 1.1 seconds. This excitation signal was imported to Tracktion, where it was duplicated three times with a small time period of silence between each single sweep.

The probes were assigned a channel each in Tracktion and the signals were recorded while the three sweeps were played. Both the voltage at the woofer and the current at the tweeter were saved as WAV files and imported in MATLAB in order to calculate the transfer function.

A WAV file has a full scale amplitude range from -1 to 1 which represents the scaled down voltage or current in these measurements. The scaling factor was unknown so it had to be measured, which was done by running the impedance measurement software LoadEd, written by Lab.gruppen. A known load of 4 Ω was connected to the amplifier and a voltage of 2 V was applied at the output by LoadEd, which ideally gives a current of 0.5 A. The probes were set to measure the voltage and the current, resulting in waveform levels at 0.0023 for the voltage and 0.00058 for the current. Hence, the resulting scaling factors were approximately 870 for the voltage and 862 for the current. It is probable that the scaling factor for the current is also set to 870 since it only deviates by 0.9 %, which should be within the error tolerance of the load.

3.3 Transfer Function Estimation

In order to be able to compensate the coupling a transfer function has to be estimated as in (11) where; V_{LF} is the frequency domain representation of the voltage over the woofer and V_{HF} is the corresponding induced voltage at the tweeter.

$$H = \frac{V_{HF}(f)}{V_{LF}(f)} \tag{11}$$

Since the known signal is the current of the tweeter, an estimation of the corresponding voltage is needed. This is done by measuring the impedance Z_{HF}, from which the voltage can be obtained by Ohm's law leading to the relation given in (12), where; I_{HF} and V_{HF} are the frequency domain representation of the current and voltage across the tweeter respectively.

$$H = \frac{Z_{HF}(f)I_{HF}(f)}{V_{LF}(f)} \tag{12}$$

The first measurements were done on the voltage across the woofer and induced current through the tweeter. Three sweeps were used as excitation signal, as described in Chapter 3.2. The last two of these was correlated, added and divided by two, so that the variations from the noise could be reduced. The resulting voltage across the woofer is shown in Figure 9 and the coupled current through the tweeter is shown in Figure 10.

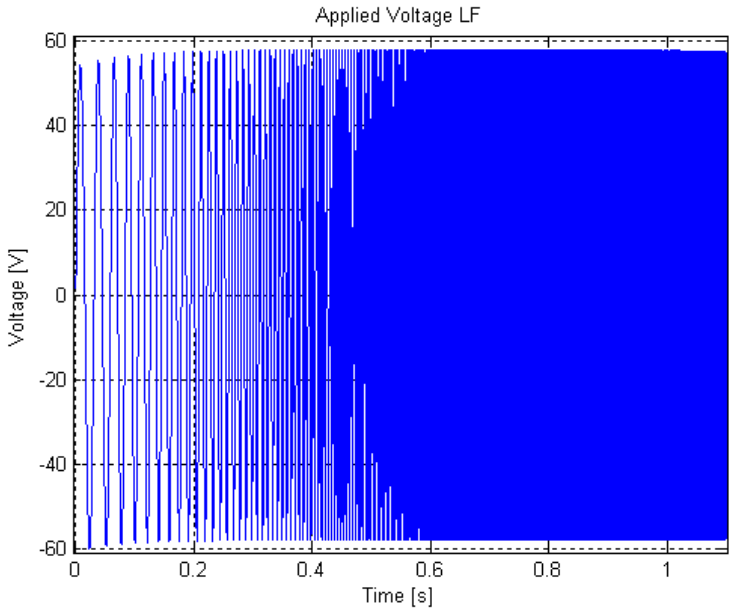

Figure 9: Applied voltage across the woofer with a logarithmic excitation signal.

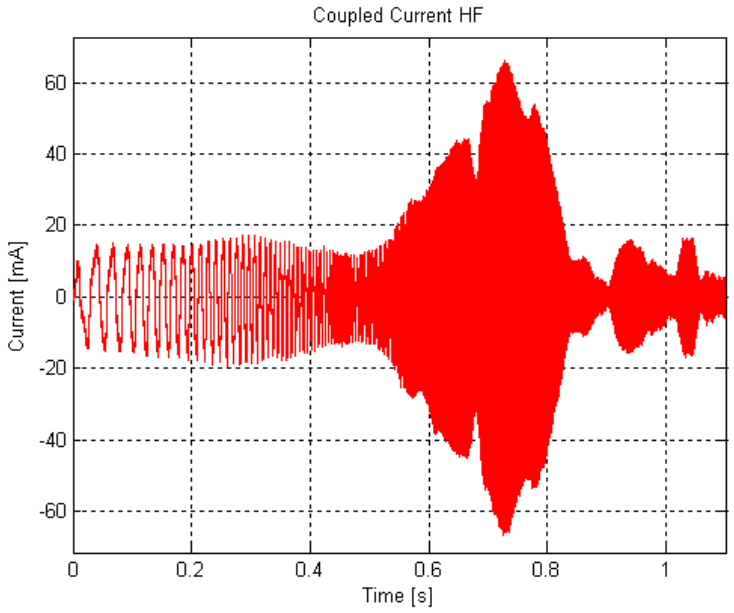

Figure 10: Coupled current through the tweeter when the voltage in Figure 9 is applied at the woofer

It can be seen in Figure 9 that the applied voltage has a transient in the start of the sweep. This is insignificant, since the induced current follows that envelope hence the effect is cancelled out by the division in (12). The nominal impedance of the woofer is 8 Ohm according to Table 1, which implies that an amplitude of approximately 58 V gives a peak output power at approximately $P = U^2 / Z = 420.5$ W. This is around a third of the maximum output power of the amplifier and half the continuous power rating for the woofer. Since it is necessary to know the impedance of the tweeter, the same method was used for measuring the voltage and current at the HF speaker. The voltage across the tweeter and the current through it is shown in Figure 11 and Figure 12 respectively.

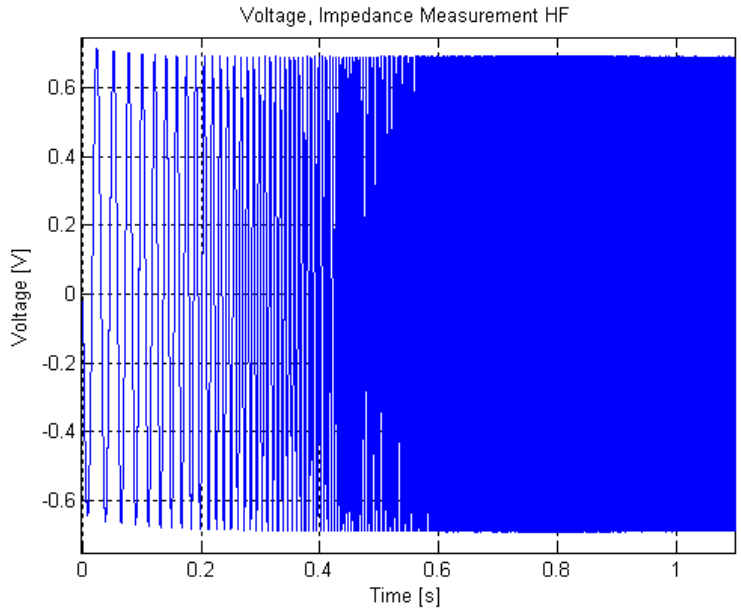

Figure 11: Voltage across the tweeter with a logarithmic excitation signal for measuring the impedance

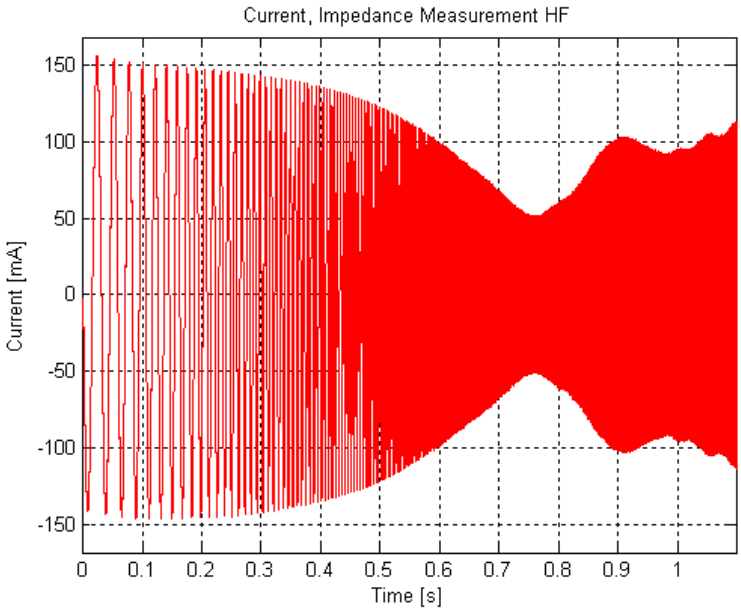

Figure 12: Current through the tweeter generated by the voltage in Figure 11.

A lower output voltage was used for the impedance measurements to avoid distortion, since the sensitivity of the tweeter is higher than for the woofer.

As it is more convenient to perform operations on the data in the frequency domain, the signals were transformed with a Fast Fourier Transform (FFT). In order to achieve lower sidelobe levels in the frequency domain, the signals were windowed. Normally a symmetric window with its center at the middle point of the time sequence is used. It is not feasible to use a window of this kind when a sweep is used, since the damping at the start and end sequence will be too high. The logarithmic increment of frequency will also demand different

tapering in the beginning and the end of the window. A custom window created to cope with this is shown in Figure 13.

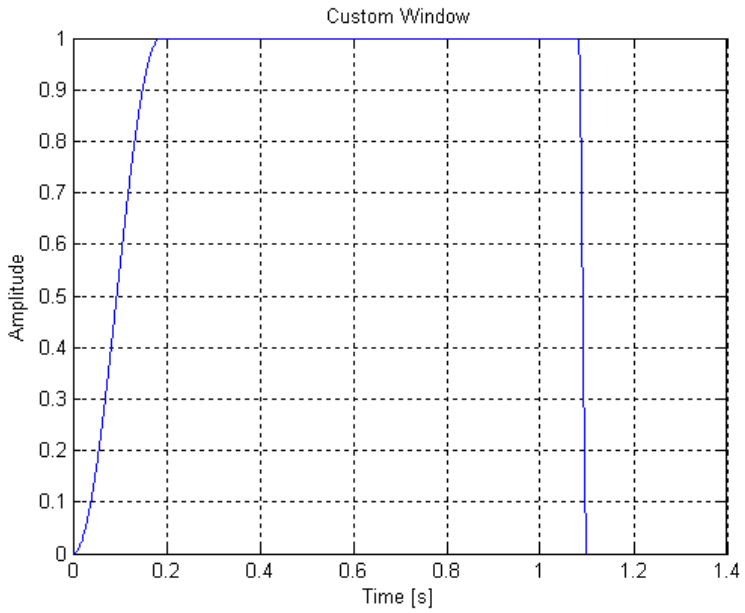

Figure 13: Custom Window used for the logarithmic signals

In order to generate the custom window, two different Hanning windows were created that have their length determined by the number of periods in the beginning and ending of the signal sequence respectively. These windows were split into two halves, and the left hand side was picked for the window intended for the beginning of the sequence. The right hand side of the other window was used for the end of the sequence. Both windows were connected with a number of ones in the middle, resulting in a total length equal to the data sequence length.

When a fast Fourier transform is used, the data sequence is always zero padded to a length of radix-2. A sequence of 1.1 seconds corresponds to a data length of 105600 at a sample frequency of 96 kHz. This gives that the closest radix-2 length is of 131072 samples. The length used for the FFT will in this report be referred to as the NFFT.

In (12), it could be seen that one division and one multiplication has to be done in the frequency domain. This corresponds to a convolution and a deconvolution in the time domain. A signal of length m convoluted with a signal of length n gives a result with a data length of $m+n-1$ [15]. If both signals are assumed to have the length n, it follows that the result from a convolution will be of length $n+n-1=2n-1$. If two convolutions are going to be calculated in the time domain, the total length of the result will therefore be $2n-1+2n-1=4n-2$. When $\mathrm{n}=105600$, as for the analyzed data length, the total number of samples after the operations will correspond to $\mathrm{k}=422398$. If a time sequence of length k is transformed into the frequency domain using a FFT, it will be zero padded to a length of $\mathrm{NFFT}=524588$, which is 4 times higher than the NFFT required for a sequence of length n. This is the minimum length that has to be used but in order to avoid any aliasing artifacts. An even higher NFFT size of 2097152 was used since the effect of the octave band averaging used in the impedance calculation was unknown.

All windowed signals were transformed into the frequency domain using an NFFT length of 2097152, and divided by the signal length n = 105600. The result is shown in Figure 14 for the coupling measurement and in Figure 15 for the impedance measurement of the tweeter in the frequency range 30 Hz to 3 kHz.

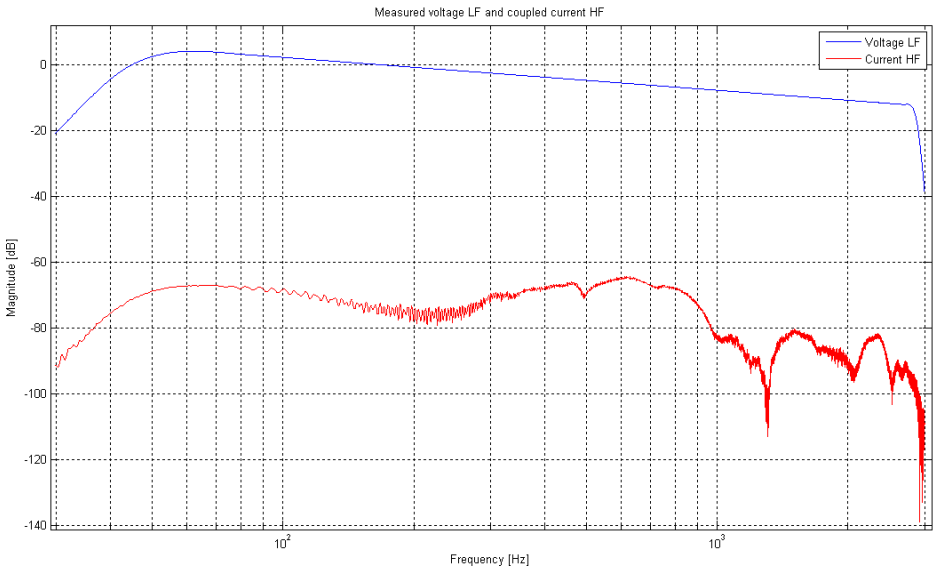

Figure 14: Voltage LF and coupled current HF from 30 Hz to 3 kHz

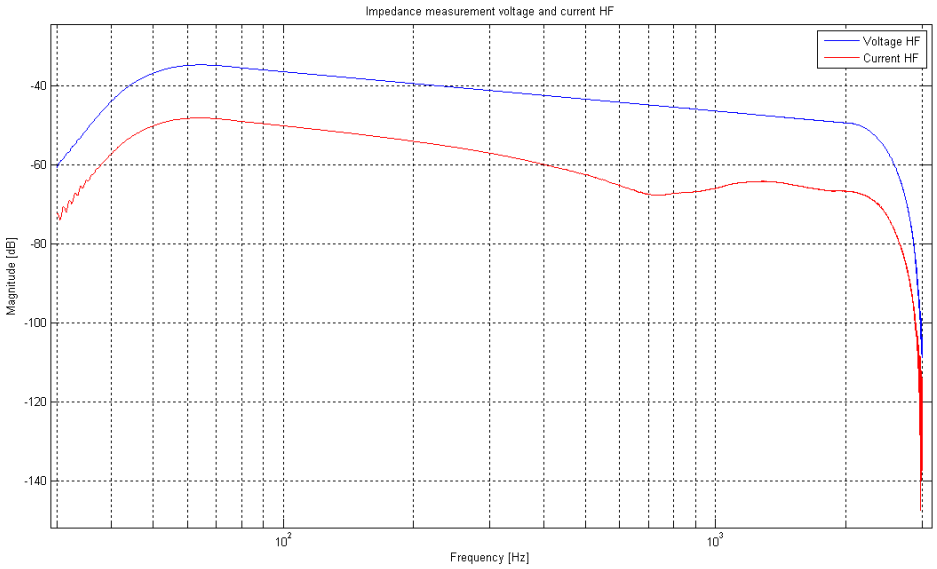

Figure 15: Voltage and current for the impedance measurement at the HF from 30 Hz to 3 kHz

As anticipated the magnitude drops by 3 dB/octave or 10 dB/decade. The impedance of the tweeter was calculated using Ohm's law $Z_{HF} = U_{HF} / I_{HF}$ and smoothed by calculating the average value of the components around each 1/8th octave band. The result is shown in Figure 16.

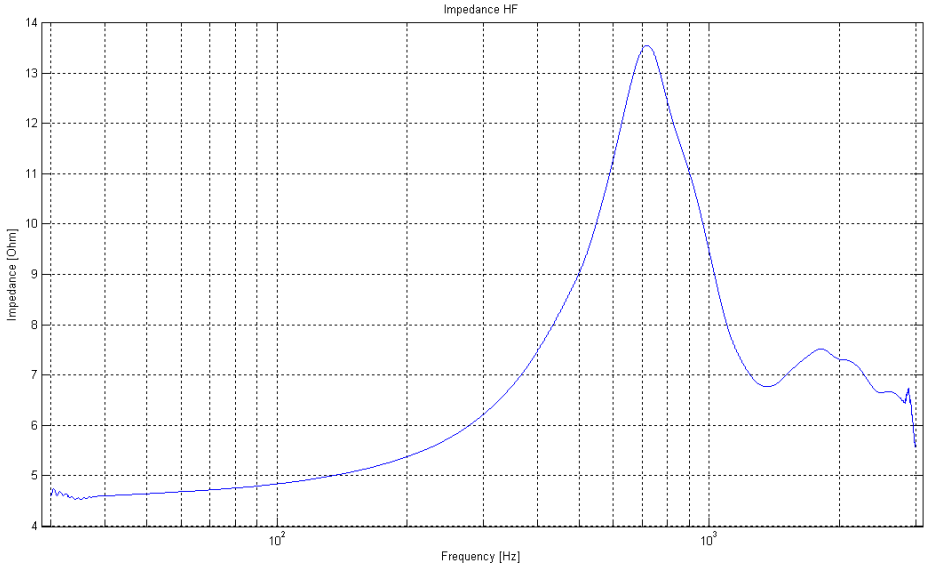

Figure 16: Impedance of the HF averaged around each 1/8th octave band

It can be seen in Figure 16 that the calculated impedance differs from the LoadEd measurement in Figure 5. This is because the voltage across the tweeter is estimated rather than measured in LoadEd. The estimation gives rise to erroneous values at higher frequencies.

The transfer function I_{HF}/U_{LF} was calculated and multiplied with the impedance Z to obtain H. An estimation of the noise current transfer function was made by measuring the current at the tweeter with no signal applied. These results are shown in Figure 17.

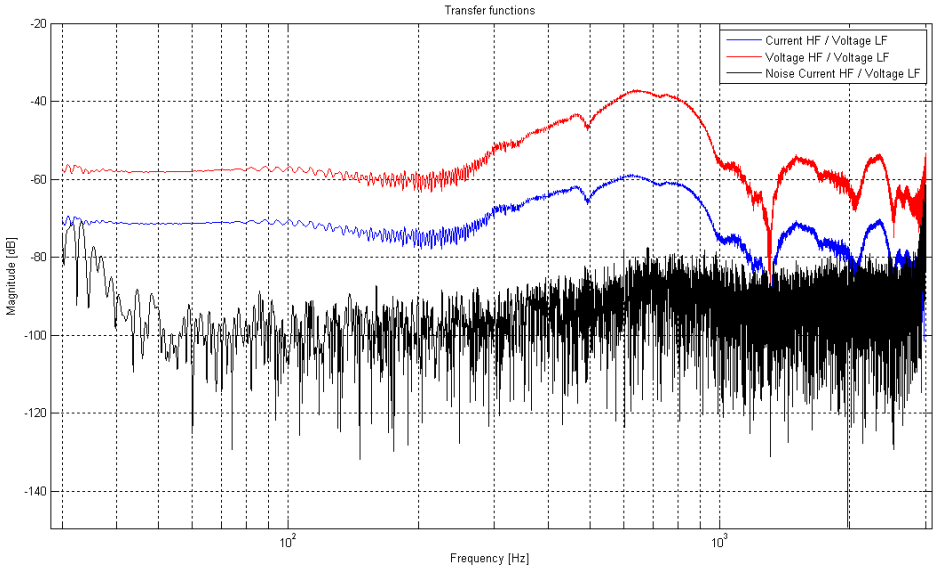

Figure 17: Transfer functions and noise floor

The transfer function H is only valid from approximately 60 Hz because of the windowing. Since the cross-over frequency is located at 1.2 kHz, the coupling above the notch at 1300 Hz can be disregarded. For this reason high- and low-pass Butterworth filters were

created with cut-off frequencies at 45 Hz and 975 Hz respectively. The order of the filters was set to 0 for the high-pass filter and 8 for the low-pass filter so that they follow the characteristics of the transfer function. These filters were used to extend the frequency response of the transfer function. It should be noted that a high-pass filter of order 0 corresponds to an all-pass filter.

Windows that mix the high/low-pass filters and the transfer function H were created to avoid discontinuities. The windows were created by splitting a Hanning window into two parts. Each part has the length of the number of bins the mixing region covers. The windows in the frequency range 67 Hz to 85 Hz are shown in Figure 18.

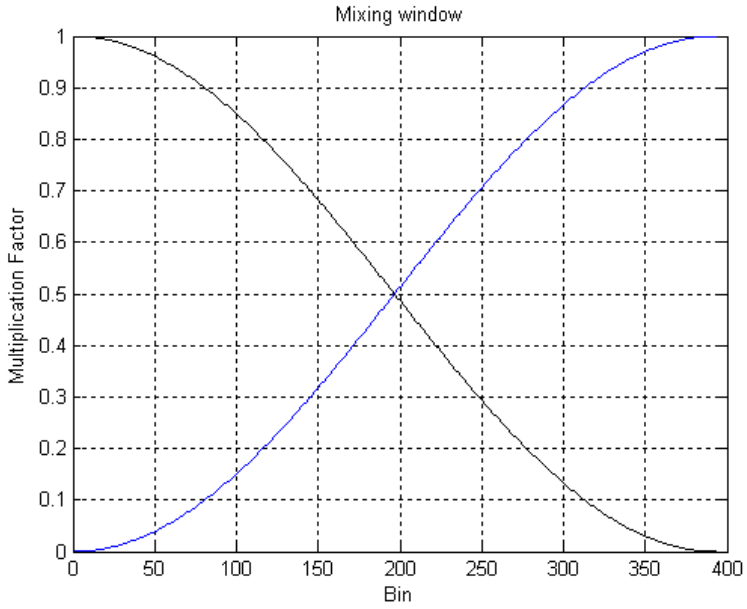

Figure 18: Mixing window from 67 Hz to 85 Hz

The low-pass filter was mixed between the frequencies 1200 Hz and 1300 Hz. Hence the modified transfer function consists of a high-pass filter from DC to 66 Hz, a mixing region between 67-85 Hz, the transfer function H from 67-1199 Hz, a mixing region from 1200-1300 Hz and a low-pass filter from 1301 Hz to the Nyquist frequency at 48 kHz. The resulting frequency response is shown in Figure 19.

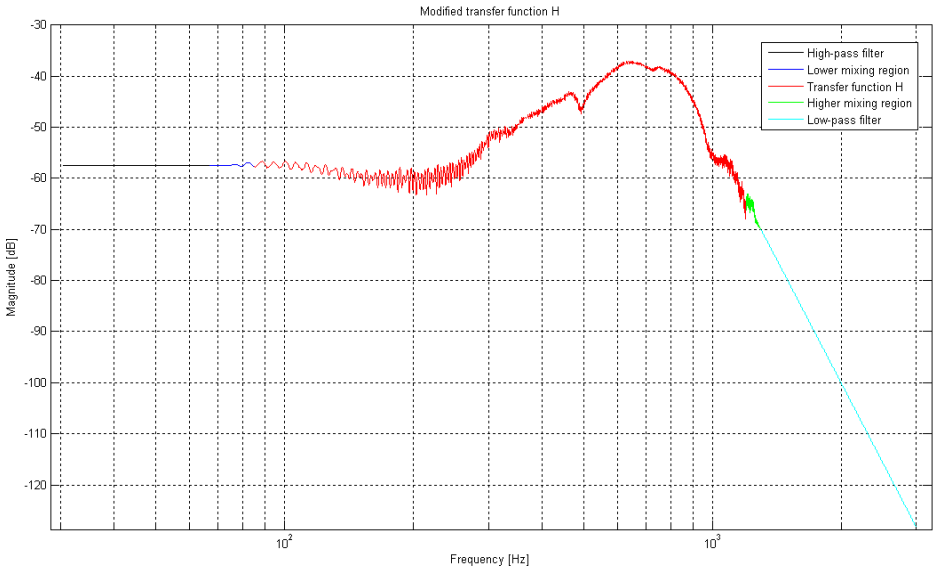

Figure 19: Modified transfer function H

It could be seen in Figure 19 that the compensation is valid from 80 Hz to 1.2 kHz. The phases for the high-pass filter, transfer function and low-pass filter were unwrapped, so that the phase offset of the high-pass and low-pass filter could be calculated. By adjusting the offset it is assured that the low-pass and high-pass filter has made the same amount of turns as the transfer function around the polar coordinate system axis. Adjustments of the phase offsets for the low- and high-pass filter were done according to Equation (13), where Φ is the phase of the low- or high-pass filter in radians, f is the frequency in Hz, Φ_H is the phase of the transfer function in radians and f_0 is the frequency where the number of turns around the polar axis should be equal.

$$\Phi(f) = f \cdot \left[\Phi(f) + \Phi_H(f_0) - \Phi(f_0)\right] / f_0 \qquad (13)$$

With f_0 chosen as the middle frequency for the mixing regions the resulting unwrapped phase is equal to that shown in Figure 20.

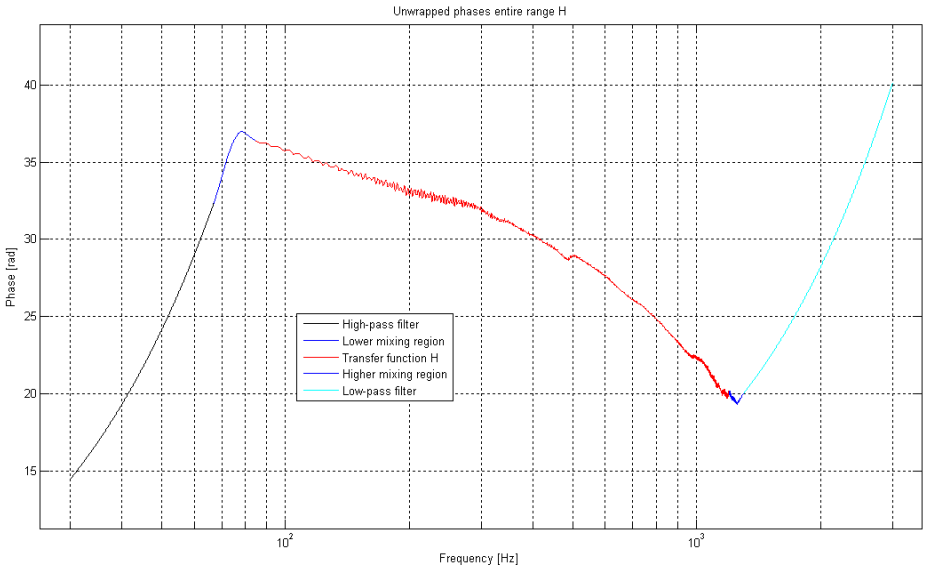

Figure 20: Unwrapped phases

It can be seen in Figure 20 that the phase of the low-pass filter does not follow the characteristics of the phase of the transfer function, which it ideally should. This has no significance since the magnitude is decreasing with 160 dB/decade in the frequency range where the low-pass filter is defining the transfer function. The phase delay, defined as $\tau_d = -\Phi(\omega)/\omega$ is shown for H from 30 Hz to 3 kHz in Figure 21.

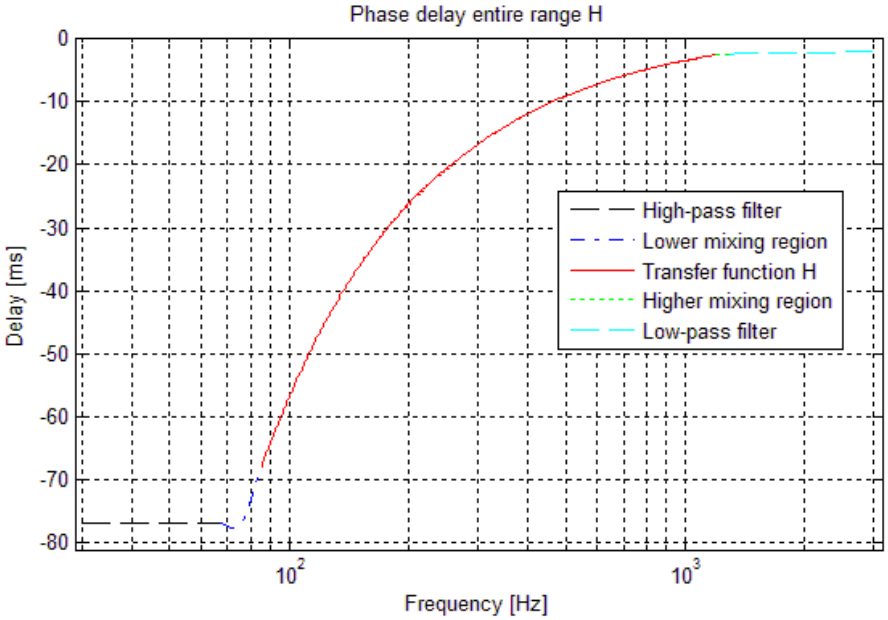

Figure 21: Phase delay from 30 Hz to 3 kHz

As shown in Figure 21, the transfer function has a non-constant phase delay, which is a consequence of the nonlinear phase in Figure 20. The magnitude and phase of the entire signal was merged by $H_{tot} = H_{mag} \cdot e^{j\angle H}$, where H_{mag} and $\angle H$ are the calculated magnitude and phase respectively. This response was inversely transformed by an IFFT (Inverse Fast Fourier Transform) with the length NFFT to obtain the impulse response h. A length of

NFFT is not feasible in practice, so the impulse response was truncated to 16632 samples and windowed at its tail between the samples 9467 to 16632 by the right hand side of a Hanning window. This gives an impulse response that is longer than necessary to keep the rounding error low in the verification. The result from 1 to 3000 samples is shown in Figure 22.

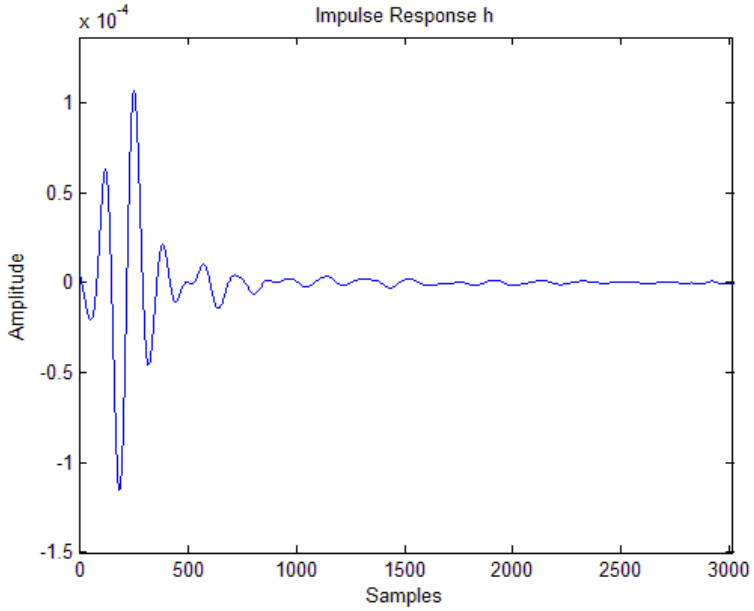

Figure 22: Impulse response h for the compensation filter

3.4 Adaptive Filter Solution

An adaptive filter is a filter that adjusts its impulse response according to an algorithm to minimise an error function. The optimal solution is given by the Wiener filter, which requires detailed information about the system and the signal environment. It is also computationally heavy, which opts for a solution that is faster but still converges to values that are sufficiently close to the optimum. The most commonly used adaptive algorithms for this purpose are the RLS (Recursive Least Squares) and LMS (Least Mean Squares). An RLS filter with N taps has a computational load of 10N+1 multiplications, 9N+1 adds/subtractions and 2 divisions while an LMS filter with the same amount of taps requires 2N multiplications, 2N adds/subtractions and no divisions [15]. The RLS algorithm converges faster and to a more accurate solution than the LMS algorithm [15]. In Chapter 3.3 the resulting number of taps N of the calculated filter is in the order of thousand samples, hence an LMS algorithm has been chosen to reduce the computational load.

The adaptive system that was used to estimate the transfer function is shown in Figure 23, where *e(t)* is the error signal, *y(t)* is the current through the tweeter, *x(t)* is the voltage across the woofer and *h(t)* is the estimated filter.

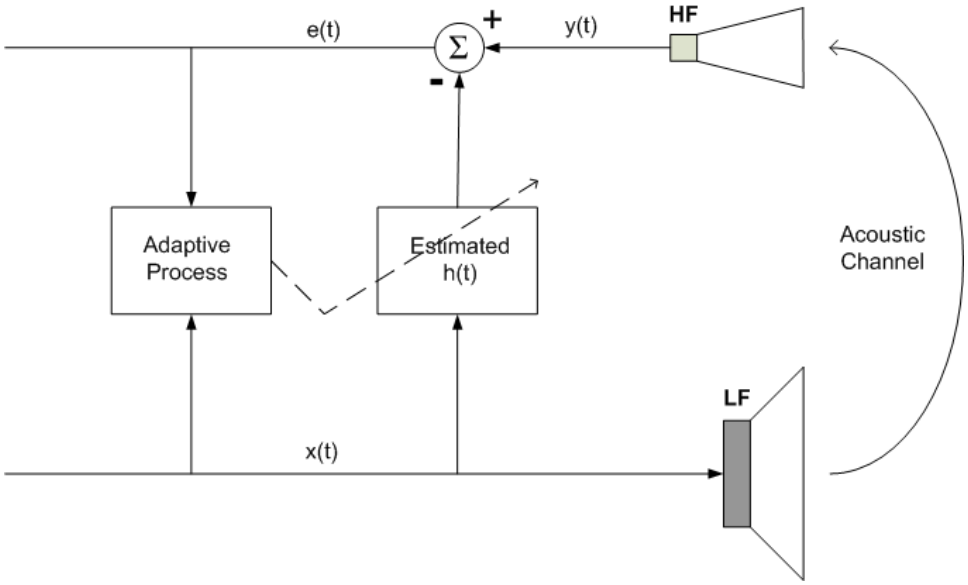

Figure 23: Block diagram of the adaptive system

It is important to notice that this system is only valid when no signal is applied at the tweeter. A low-pass filter could be inserted after the current probe in a real case scenario to suppress the influence of the HF signal. The objective of the LMS algorithm is to minimise the error *e(t),* which is done in the least mean square sense, as implied by its name. Let $\vec{h}(n)$ denote the filter vector at the sampling instance n and $\vec{x}(n)$ be a vector of input data with the same length as the filter vector. The first step of the algorithm is to initialise the filter by setting $\vec{h}(0) = 0$. The filter is then updated for each sample $n = 1, 2, \ldots$ as in (14), where μ is the step length.

$$\begin{aligned} \hat{y}(n) &= \vec{h}^{\,T}(n-1)\vec{x}(n) \\ e(n) &= y(n) - \hat{y}(n) \\ \vec{h}(n) &= \vec{h}(n-1) + 2\mu\vec{x}(n)e(n) \end{aligned} \tag{14}$$

The choice of step size is dependent on the eigenvalues of the covariance matrix of the input signal, which in a practical situation is impossible to calculate [15]. A step size range which is more practical is given in (15), where; N is the number of filter taps and $\sigma_x^2 = E\left[x^2(n)\right]$ is the variance of the input signal.

$$0 < \mu < \frac{1}{3N\sigma_x^2} \tag{15}$$

A practical choice is to set the step size at the middle of this range namely at $1/6N\sigma_x^2$. The same sweep that was used to estimate the transfer function in Chapter 3.3, was also used as a training signal for the adaptive filter. Code for the LMS algorithm was entered in MATLAB and the filter length was empirically set to 8000 samples. An excitation signal of a logarithmic sweep from 30 to 30 kHz gave the step size $\mu \approx 1.24 \cdot 10^{-8}$. The algorithm was run a total of two times, one time with the second sweep measurement as input signals and one time with the third sweep. This resulted in the impulse response shown in Figure 24. Note that this is the filter for the transfer function from the voltage across the woofer to the current through the tweeter.

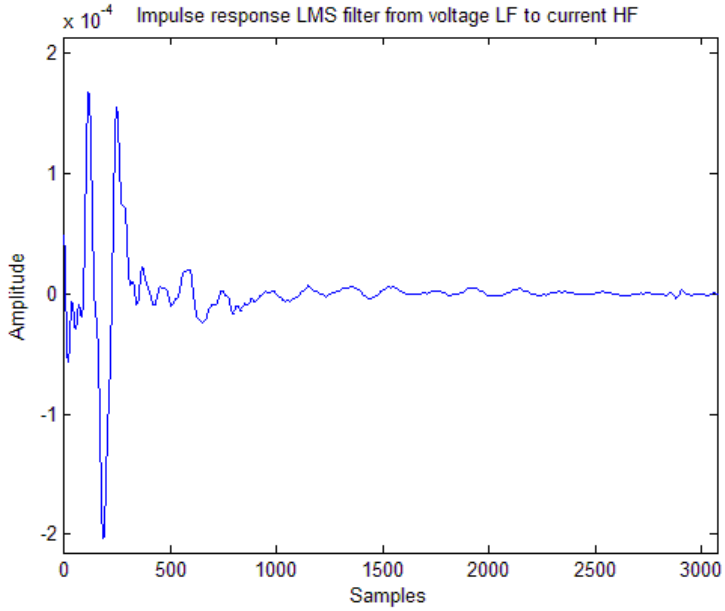

Figure 24: Impulse response generated by the LMS algorithm

The impulse response generated by the LMS algorithm and the impedance measurement was transformed into the frequency domain by an FFT of length 262144 using the same method as in Chapter 3.3. Since the magnitude of the LMS filter could vary while it is updated the frequency range was extended for the impedance of the tweeter instead. High- and low-pass filters were designed for defining the low and high frequency spectra of the impedance with cut-off frequencies at 34 Hz and 1835 Hz respectively. The order of the high-pass filter was set to 0, which makes it an all-pass filter. The generated low-pass filter was of the 1th order. The mixing regions were defined between 40 - 50 Hz and 2700 - 2950 Hz. Figure 25 shows the resulting impedance from 30 Hz to 4 kHz.

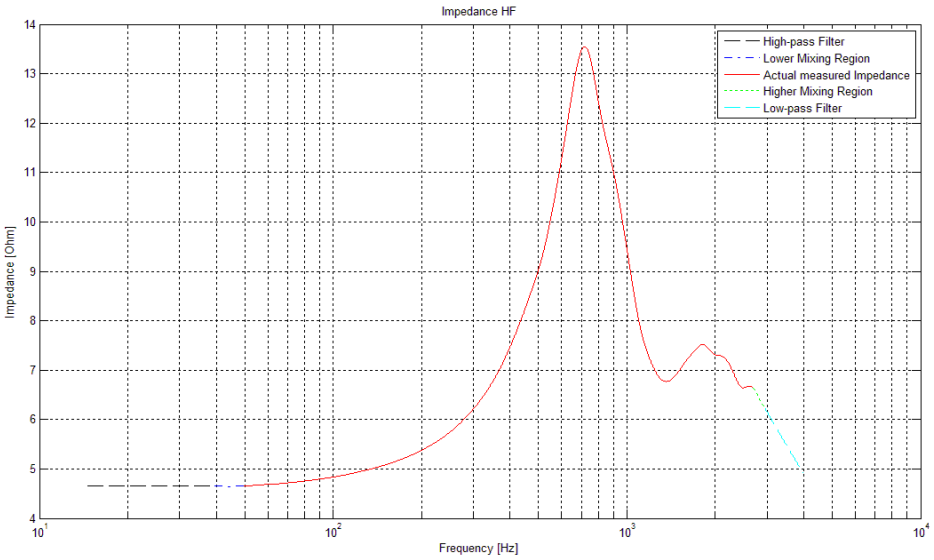

Figure 25: Impedance of the HF with extended low and high frequency response

A transfer function from the voltage at LF to the voltage at HF was calculated by multiplying the LMS filter with the impedance. The resulting filter H and the previously transformed LMS filter is shown in Figure 26 from 30 Hz to 3 kHz

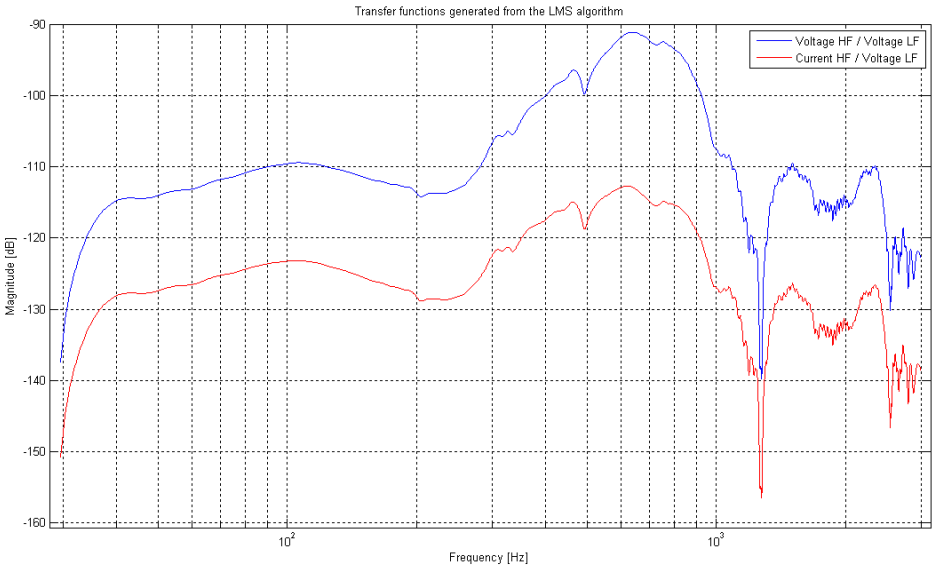

Figure 26: Transfer functions generated from the LMS algorithm

It can be seen in Figure 26 that the characteristics of the transfer function agree with the estimated transfer function in Figure 17. The magnitude is a bit smoother in Figure 26, which could be explained by the difference in frequency resolution, whereas a lower NFFT was used for the adaptive filter resulting in a lower resolution. The reason of the magnitude offset between the adaptive filter solution and the estimated transfer function is that an FFT is done directly on the impulse response generated by the LMS algorithm. A plot of the phase response for the LMS voltage transfer function from 30 Hz to 3 kHz is shown in Figure 27.

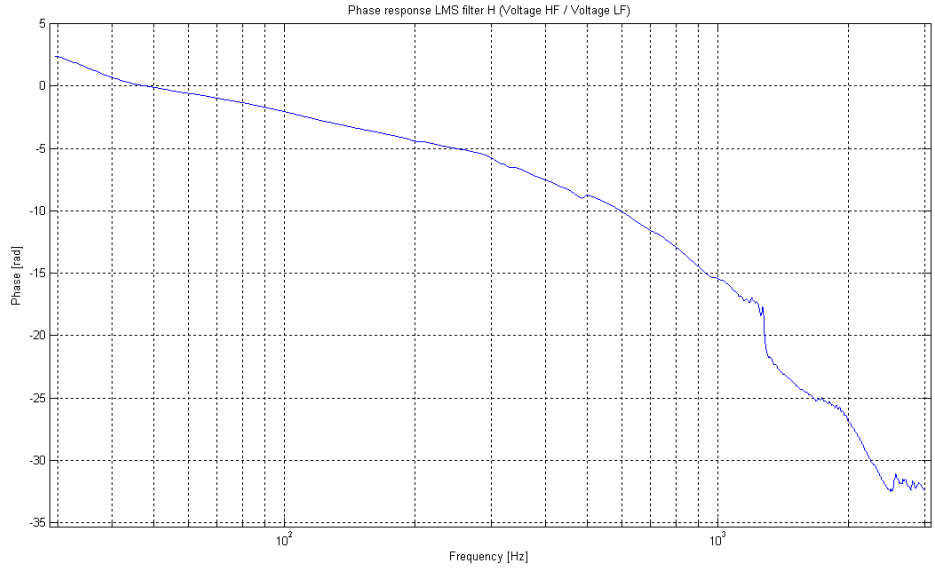

Figure 27: Phase response, LMS filter H

The phase response in Figure 27 has a smoother appearance than the previously estimated response in Figure 20. This is probably due to the frequency resolution as with the magnitude. An IFFT was done on the total response of the calculated transfer function with the same length as the NFFT, resulting in the impulse response shown in Figure 28 from 1 to 3000 samples. A total filter length of 8000 samples with Hanning windowing from 6000 to 8000 samples was found to give a good compensation.

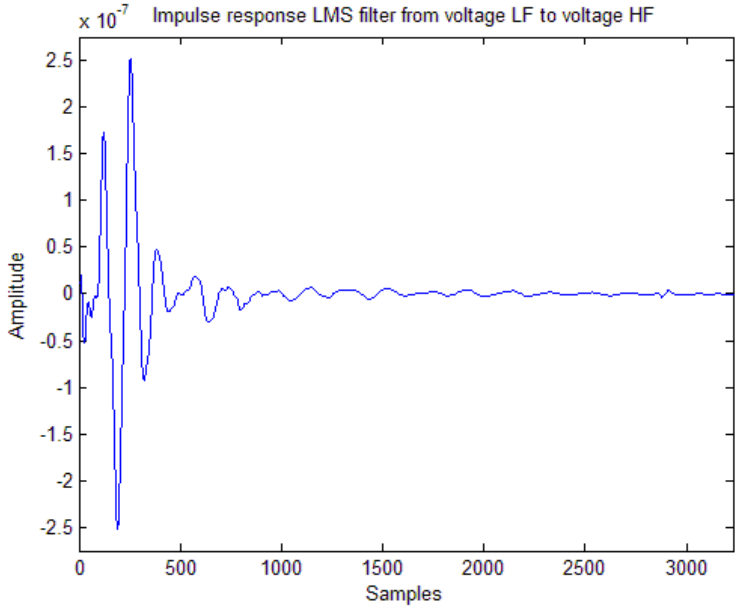

Figure 28: Impulse response LMS filter from voltage LF to voltage HF

It is apparent that the impulse response in Figure 28 is very similar to that in Figure 22, except in the beginning of the sequence. The ability of compensating the induced current is given account for in Chapter 5.1.

3.5 Generating the equalizers for the JBL SRX712M

The equalizer settings that were used to get a straight frequency response were taken from an audio processor with data for the JBL SRX712M. Linkwitz-Riley filters with a slope of 24 dB/octave and crossover frequencies at 50 Hz and 1.3 kHz defines the band-pass for the woofer along with a gain of 3 dB. A total of 7 parametric filters were also used to characterize the frequency spectrum, whose parameters are given in Table 3.

Table 3: Parametric filters for the woofer

Frequency [Hz]	Gain [dB]	Q-factor
70	3	2.654
180	-7	10
215	6.5	1.356
730	-3	3.857
500	-3	4
350	-3	7.5
885	-1	8

The band-pass filter for the tweeter is defined by two Linkwitz-Riley filters with slopes of 24 dB/octave and crossover frequencies at 1.4 kHz and 20 kHz with a total gain of -12.5 dB. Totally 8 parametric filters defines the equalization of the tweeter, these are given in Table 4.

Table 4: Parametric filters for the tweeter

Frequency [kHz]	Gain [dB]	Q-factor
15.4	11.5	3.875
10.9	12	7
1.85	-4.5	8
2.2	1.2	3.754
3.05	-3.5	6
4.2	-1.5	8
5.9	-3	8
9.5	-4	8

The total frequency response of these filters were generated in a software by WaveCapture called Live-Capture Pro and exported to a text-document containing the data. This data was imported into MATLAB, where it was found that it is logarithmically spaced between 10 Hz and 20 kHz with a total number of 1054 points. In order to create an impulse response from this data the entire frequency range has to be defined, so a new frequency vector was created corresponding to an NFFT length of 65536 samples. The data points between 10 Hz and 20 kHz were interpolated with respect to the new frequency range, and Linkwitz-Riley filters with the same specifications as the equalization settings were created and mixed with the new response to define the magnitude below 10 Hz and above 20 kHz. An extra gain of 3 dB was added for the woofer and a gain of -12.5 dB for the tweeter. Figure 29 shows the result for the LF and Figure 30 for the HF.

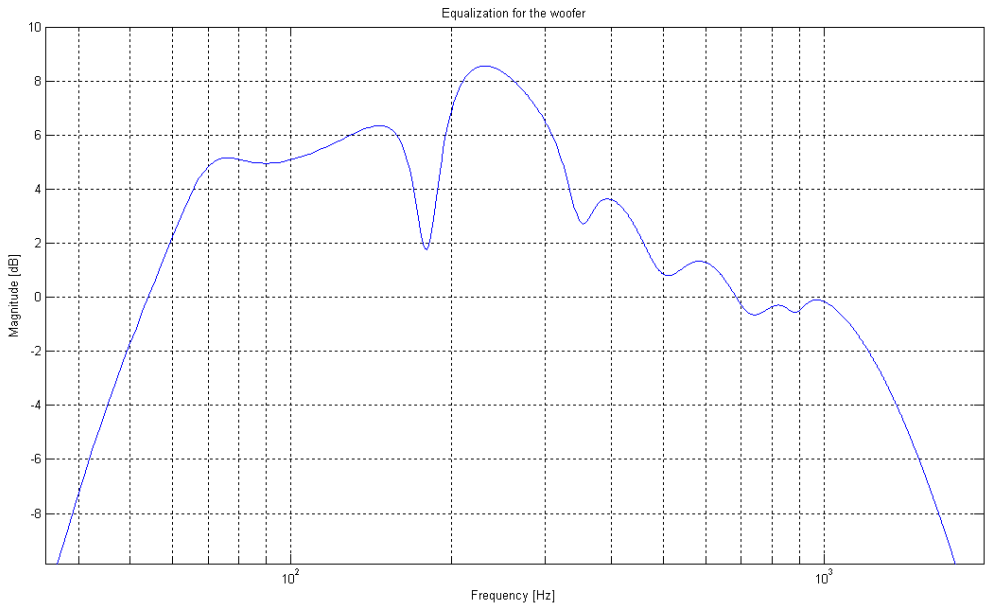

Figure 29: Frequency response of the generated equalization for the woofer in the JBL SRX712M

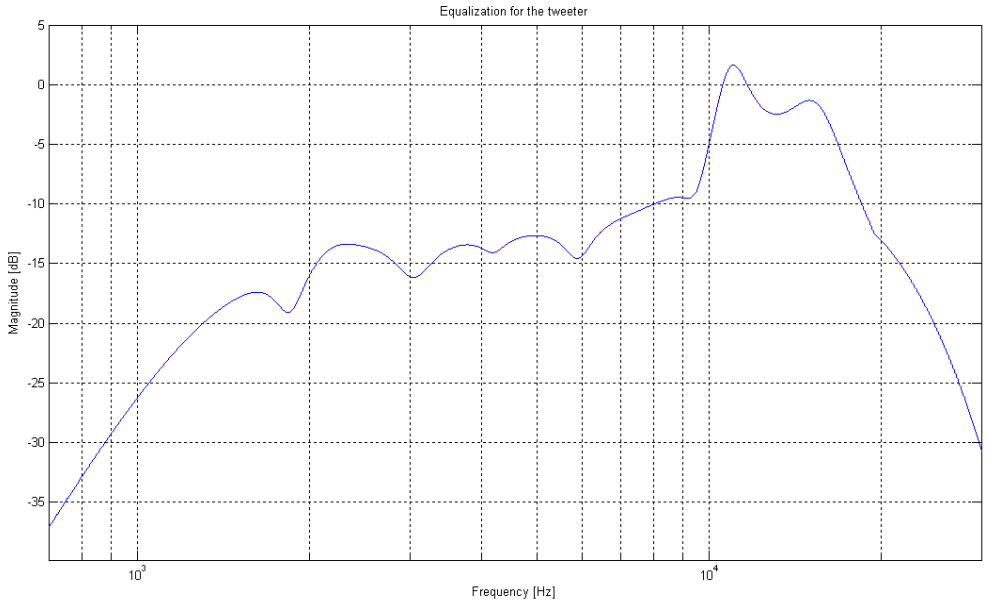

Figure 30: Frequency response of the generated equalization for the tweeter in the JBL SRX712M

The power spectrum for each equalizer setting was transformed into the time domain to an impulse response with a minimum phase group delay. These impulse responses were truncated at 8000 samples, where the amplitude for the LF was close to the LSB of a 24-bit quantization. A Hanning window of 1000 samples was created, and the right hand side of 500 samples was used to window the tail of the impulse responses. A delay of 63 µs was introduced for the LF by inserting 6 zeros in the beginning of the impulse response.

4 Implementation in AlgoFlex

AlgoFlex is a software developed by TC Electronic which allows the user to test audio processing algorithms. It is a block based system, where each block is built from C/C++ code and connected in a processing chain. The main application is a server, to which the binaries from the blocks and their connections are uploaded and run by the engine at a sample-rate basis. A java client and MATLAB are used to communicate with the server, where the main code is entered in MATLAB.

A number of pre-built standard blocks are included in AlgoFlex, these were sufficient for implementing the compensation algorithm. The following standard blocks were used;

- **Audio I/O** - Configures the audio input and output routing through the desired recording/playback device.
- **FilePlayer** - Plays the audio samples from a sound file.
- **Gain** - Attenuates or amplifies the signal with a constant gain.
- **FastConv** - Implements one or more FIR filters, where the desired impulse response is entered
- **Limiter** - A simple limiter, which in the compensation algorithm is used to attenuate the signal with a constant gain if it is above a certain threshold value
- **ChannelCombiner** - Used to sum two signals.

The impulse responses generated by the method described in 3.5 were loaded into a FastConv block with two outputs to create the equalizers. A compensation filter H was created with the same method, using the calculated impulse response. The output of this filter will have an unknown latency that is dependent on the implementation method of the FastConv block. Therefore two delay blocks were created by loading a unit impulse function with the same length as the compensation filter into a FastConv block, named "Delay HF" and "Delay LF". The total system setup for one channel (Left or Right in a stereo setup) is shown in Figure 31.

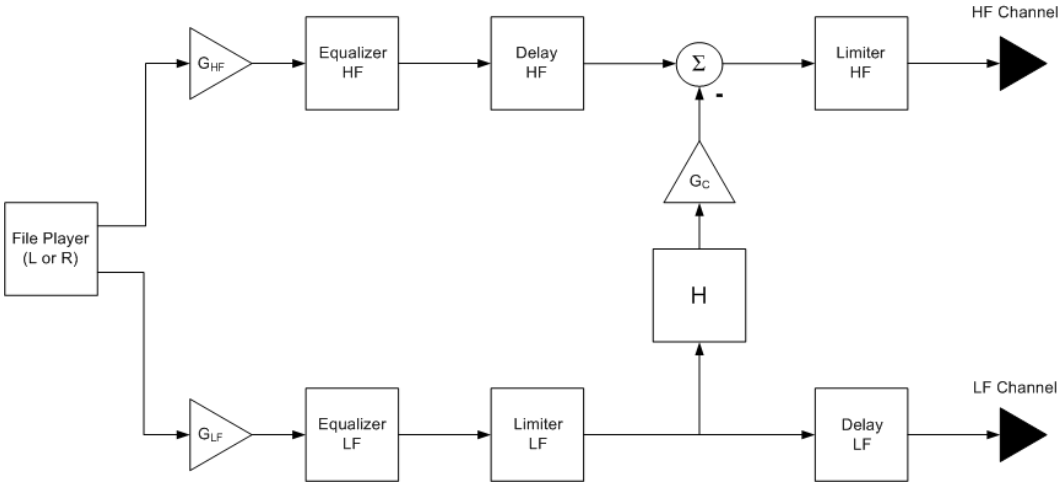

Figure 31: Setup in AlgoFlex

In Figure 31, the HF channel and LF channel are connected by the Audio I/O block to the MOTU 828mkII sound card. The subtraction after the compensation gain G_C, is done by negating the impulse response of the filter H. The gain for the compensation was found empirically by measuring the induced current, the compensating current and the compensated current. The file player can also be exchanged to the Audio I/O block inputs if an external sound source is to be used.

5 Verification

This chapter reviews how well the compensation works, where comparisons of the induced current is done for the system without and with compensation. Distortion measurements with and without compensation for the JBL SRX712M are given account for, as well as the listening test for the same speaker.

5.1 Compensation Measurement

Measurements of the compensation were done by running the algorithm developed in AlgoFlex at an output level of 11.2 V at the woofer with the tweeter inactive. AlgoFlex was connected using ASIO drivers through firewire to the MOTU soundcard, whose analog outputs were connected to the analog inputs of the PLM10000Q. The voltage across the woofer and current through the tweeter were both transmitted to another computer through Dante, where they were recorded with Tracktion. This setup is shown in Figure 32.

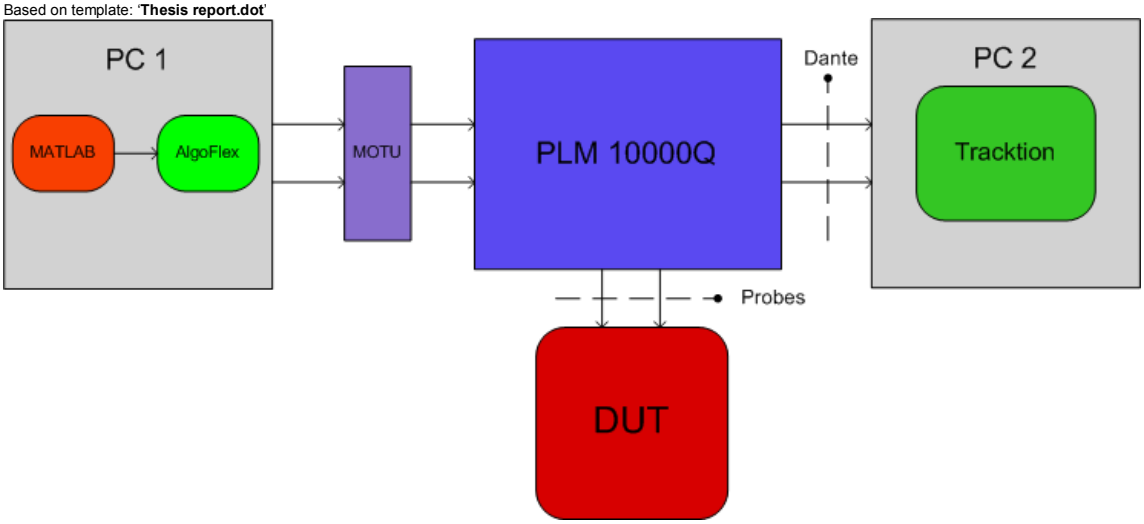

Figure 32: Measurement setup used for the verification. Note that the probes are located inside the PLM

Both the estimated transfer function described in Chapter 3.3 and the adaptive filter solution from Chapter 3.4 was tested. These measurements were done at Lab.gruppen with another JBL SRX712M than the one used in Chapter 3, so the characteristics of the transfer function differs. The same measurement method as in Chapter 3 was used, but only the second sweep is examined in the following parts. In Figure 33, the induced current and the compensated current for the estimated transfer function are plotted and synchronized for comparison.

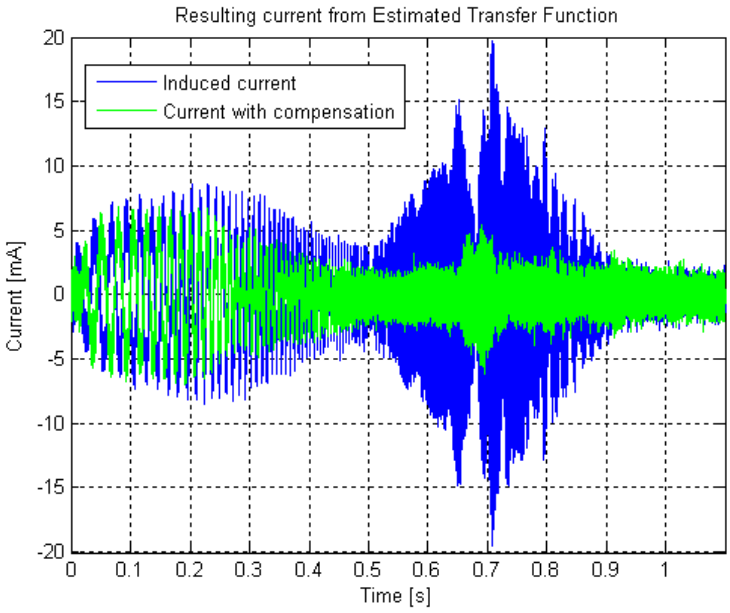

Figure 33: Induced and compensated current with the estimated transfer function

It can be seen in Figure 33 that the compensation level at the beginning of the sequence is lower than in the remaining sequence. The induced current is also less damped in the region from 0.65 to 0.7 seconds. These discrepancies are more easily explained by examining the sequence in the frequency domain. The induced current, compensated current, noise current and the compensating current was transformed into the frequency domain along with the voltage. The transfer functions from the voltage across the woofer to the current through the tweeter were calculated, resulting in the spectrum shown in Figure 34.

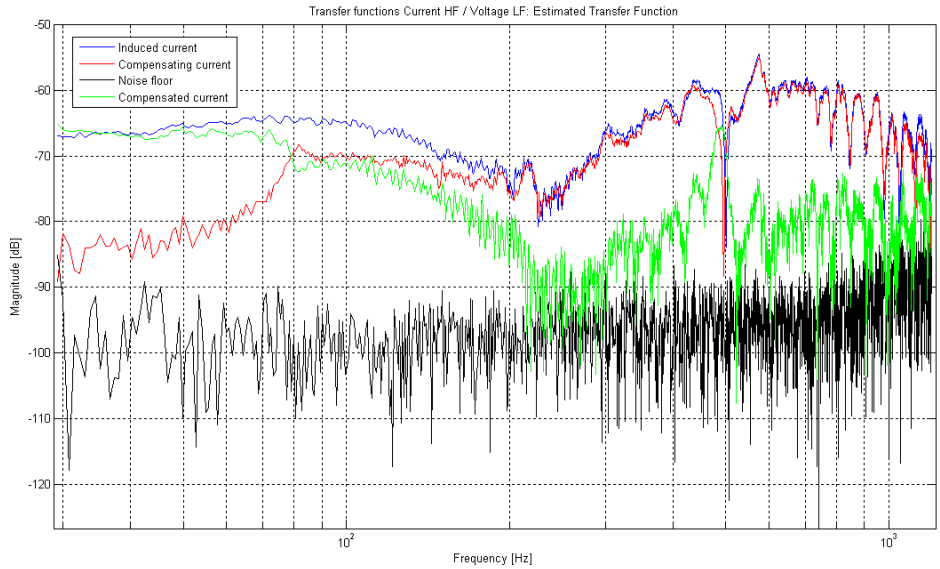

Figure 34: Magnitude of the transfer function for the different currents using the estimated transfer function method

As can be seen in Figure 34 the magnitude characteristics resemble those in Figure 33. The lower dampening below 80 Hz is caused by the all-pass filter and the lower damping from 80 Hz to 200 Hz is probably caused by the fact that a lower voltage at the woofer was used in the verification measurement than in the transfer function measurement. It is assumed that the nonlinearities of the tweeter are more prominent at frequencies far below its resonance frequency, leading to a less effective compensation. If the magnitude of the frequency spectrum between 400 Hz and 500 Hz is inspected, it can be seen that the notch at 500 Hz has moved in frequency, which results in an over damping of the induced current around this frequency. The result from a measurement using the adaptive filter solution is shown in Figure 35.

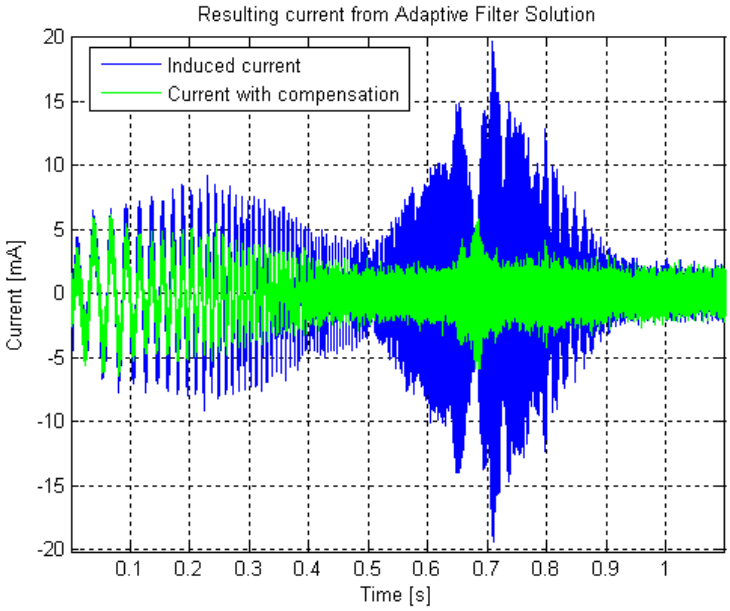

Figure 35: Induced current and compensated current with the adaptive filter solution

The amplitude of the compensated current in Figure 35 has the same areas with less damping as the compensation in Figure 33. These currents were also transformed into the frequency domain with the same method as for the analysis of the estimated transfer function. The result is shown in Figure 36.

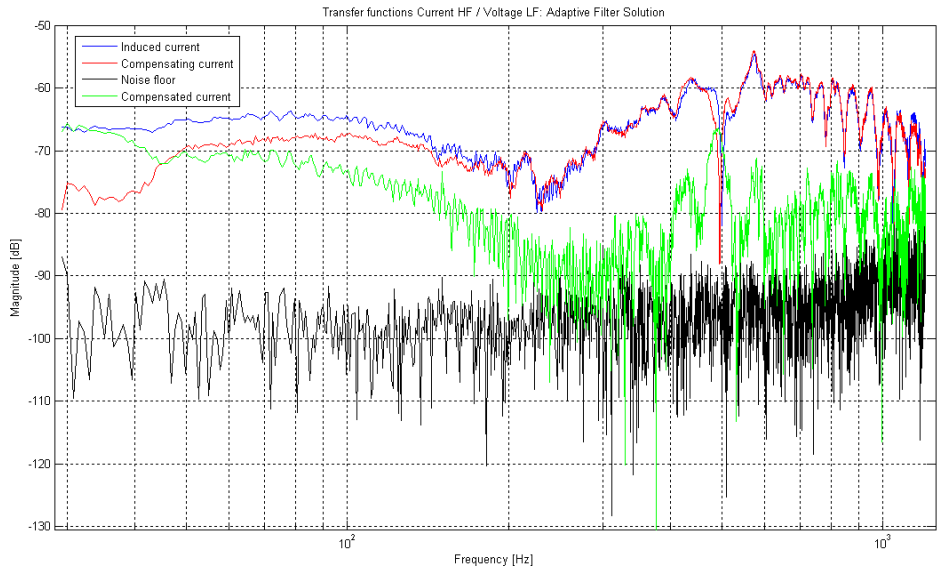

Figure 36: Magnitude of the transfer function for the different currents using the adaptive filter solution

If the magnitude of the compensated current in Figure 34 is compared to that in Figure 36 it could be seen that the damping is better in the lower frequency range, but that the notch is more over damped. Effects from the windowing are present in the region below 45 Hz. It can also be seen that the damping is less effective in areas with magnitude dips. The total damping is approximately equal for the different compensation methods.

5.2 Distortion Measurement

Distortion measurements were done in the anechoic chamber at the Division of Applied Acoustics at Chalmers University of Technology. This chamber was built in 1969 and has a sound absorption of at least 99 % in the frequency range 75 Hz to 10 kHz [17]. The used measurement setup was identical to that in the verification of the compensation, with the exception that the Behringer microphone was connected to the input of the MOTU. AlgoFlex was used to save the recorded sound from the microphone. The JBL SRX712M was placed in the middle of the room and the Behringer ECM8000 microphone was mounted on a stand at a distance of 1 m on axis from the tweeter.

A sequence of 12 tones was played on the tweeter while the woofer played the same tone 12 times simultaneously. The chosen frequency for the sinusoid at the woofer was 790 Hz. A verification of the compensation at this frequency was done, resulting in a magnitude damping of approximately 30 dB for the induced current at a peak output voltage of 15 V at the woofer. A filter generated from the estimated transfer function was used. The 12 tone sequence on the tweeter is given in Table 5.

Table 5: Tones played on the tweeter when measuring the distortion (with 790 Hz at woofer)

Tone No.	1	2	3	4	5	6	7	8	9	10	11	12
Frequency [Hz]	672	893	1105	1343	1785	2210	2686	3570	4505	5372	7140	8500

The frequencies in Table 5 were chosen by setting the start frequency at 790 Hz, calculating all 3rd octave bands up to 10 kHz and then lowering them by 15 %. The offsetting was done to be able to separate the signals from harmonic distortion generated by the tone played on the woofer at 790 Hz.

Each tone had a duration time of 32000 samples, corresponding to approximately 330 ms. A silent period of 28800 samples or 300 ms was introduced in between the tones. The sequence was played and recorded through AlgoFlex with the woofer muted. As the sound pressure level produced by the loudspeaker differs depending on the frequency of the signals, it was necessary to adjust the amplitudes of the different tones so that their levels were equal. It is important to note that this is because no equalizer was used. Their weightings are shown in Table 6.

Table 6: Tones played on the tweeter and their weightings

Tone No.	1	2	3	4	5	6	7	8	9	10	11	12
Frequency [Hz]	672	893	1105	1343	1785	2210	2686	3570	4505	5372	7140	8500
Weighting	1	0.46	0.42	0.32	0.37	0.39	0.35	0.33	0.50	0.22	0.57	0.43

A script was written to pick out the middle of the recorded sequence with a length of 8192 samples. Each part was windowed with a Hanning window and transformed into the frequency domain using an NFFT length of 8192 samples. The result of the 7th tone is shown in Figure 37.

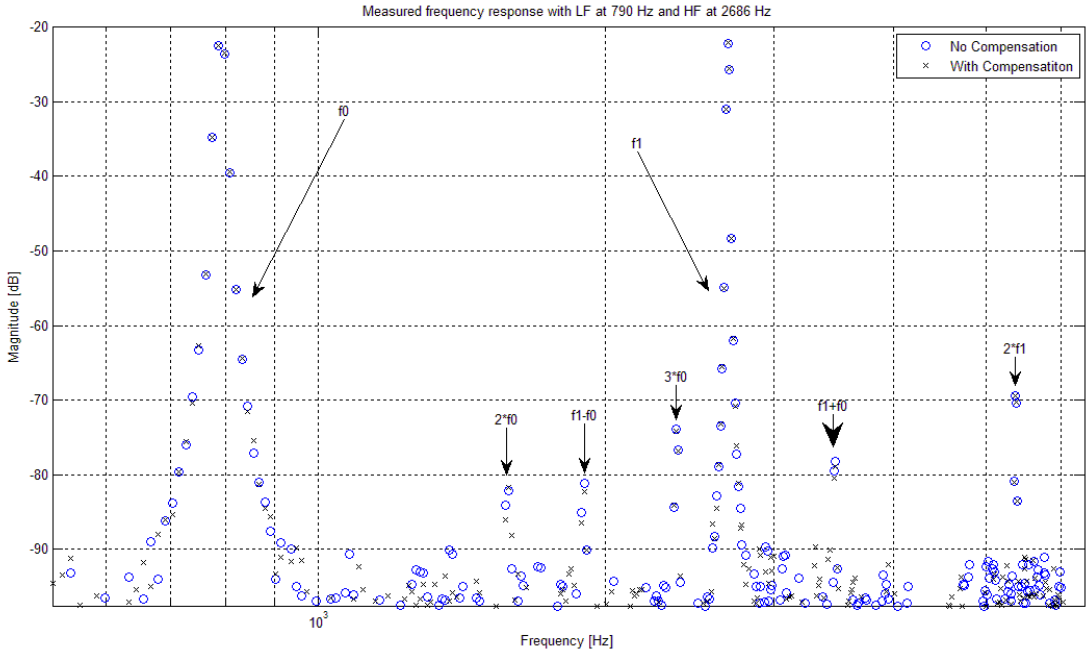

Figure 37: Frequency spectrum of the 7th measurement

The frequency components present for the 7th measurement are the fundamental of the woofer at f_0=790 Hz and its harmonic distortion components at $2f_0$=1580 Hz and $3f_0$=2370 Hz. At the tweeter, the fundamental tone is located at f_1=2686 Hz and its harmonic distortion component located at $2f_1$=5372 Hz can be seen. The most notable components in this measurement are the modulation distortion components located at f_1-f_0=1896 Hz and f_1+f_0=3476 Hz. It can be seen in Figure 37 that these components are located at approximately 60 dB and 57 dB below the f_1 component respectively. A slight damping of the modulation distortion for the compensated system is visible. This damping is easier to see in the 9th measurement which is shown in Figure 38.

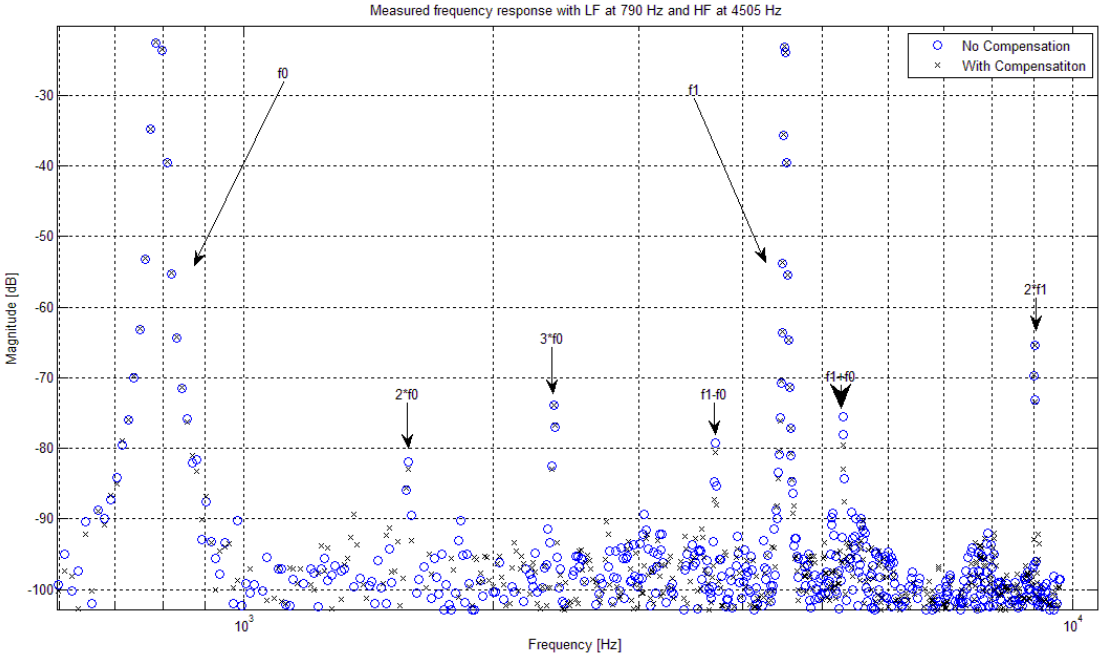

Figure 38: Frequency spectrum of the 9th measurement

The resulting frequency components in Figure 38 have the same relationship as for the 7th tone in Figure 37, but the tone at the tweeter is located at f_1=4505 Hz resulting in $2f_1$=9010 Hz, f_1-f_0=3715 Hz and f_1+f_0=5295 Hz. As seen in Figure 38 the modulation distortion components have increased in magnitude compared to the measurement in Figure 37, with levels at approximately 58 dB and 52 dB below the fundamentals. The damping of these components is also higher when the coupling is compensated. In order to give a measure of the amount of modulation distortion, the formula in (16) was used where A denotes the amplitude of the component and the TMD (Total Modulation Distortion) is given in percent. Only second order components are included, since only those have a significant contribution to the total modulation distortion in these measurements.

$$TMD = 100 \cdot \frac{\sqrt{A_{f1-f0}^2 + A_{f1+f0}^2}}{A_{f1}} \qquad (16)$$

The calculated TMD for each tone with and without compensation is shown in Figure 39.

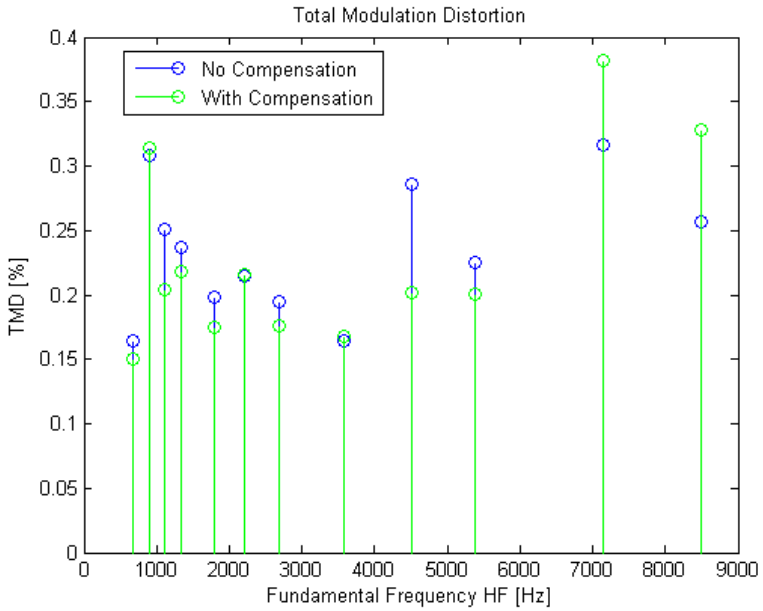

Figure 39: Total modulation distortion with and without compensation for each tone

As shown in Figure 39, the TMD is reduced with the compensation for the 1st, 3rd, 4th, 5th, 7th, 9th and 10th tone. It can be seen that the TMD is significantly increased for the 11th and 12th tone and by a smaller amount for the 2nd, 6th and 8th tone when the compensation is activated. The total harmonic distortion, THD, resulting from the tone on the tweeter was calculated as in (17), where A denotes the amplitude of the corresponding component. Harmonic distortion components up to the 4th order were included, where the THD is given in percent.

$$THD = 100 \cdot \frac{\sqrt{A_{2f1}^2 + A_{3f1}^2 + A_{4f1}^2}}{A_{f1}} \tag{17}$$

The resulting THD with and without compensation for each tone is shown in Figure 40.

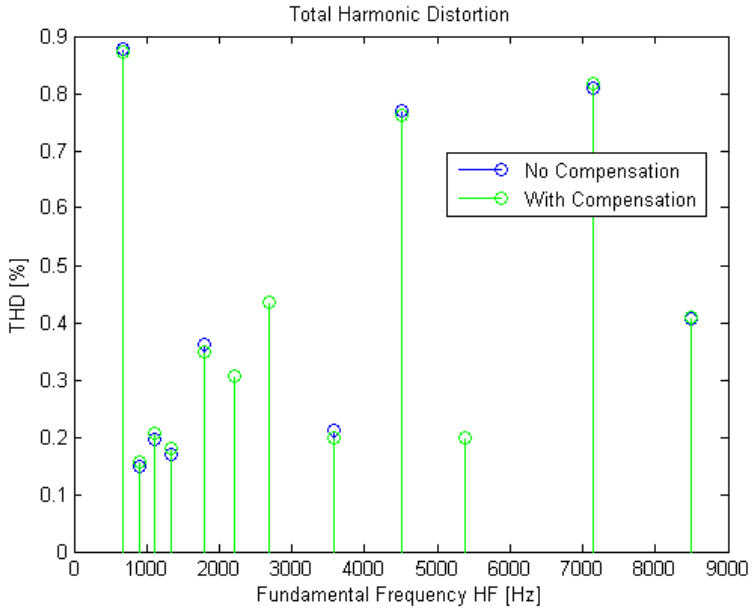

Figure 40: Total harmonic distortion with and without compensation for each tone

It can be seen in Figure 40 that the harmonic distortion for the tones on the tweeter does not differ much with and without compensation. In order to be able to calculate the dynamic range, a notch filter of Butterworth type of the 3rd order with cut-off frequencies at 732 Hz and 853 Hz was designed. The total signal to noise and distortion ratio (SNDR) was calculated as in

$$SNDR = 20 \cdot \log_{10}\left(\frac{A_{f1}}{\sum_{f=0}^{fs/2}(A_i) - A_{f1}}\right) \quad (18)$$

The resulting signal to noise and distortion ratio with and without compensation for the tone sequence is shown in Figure 41

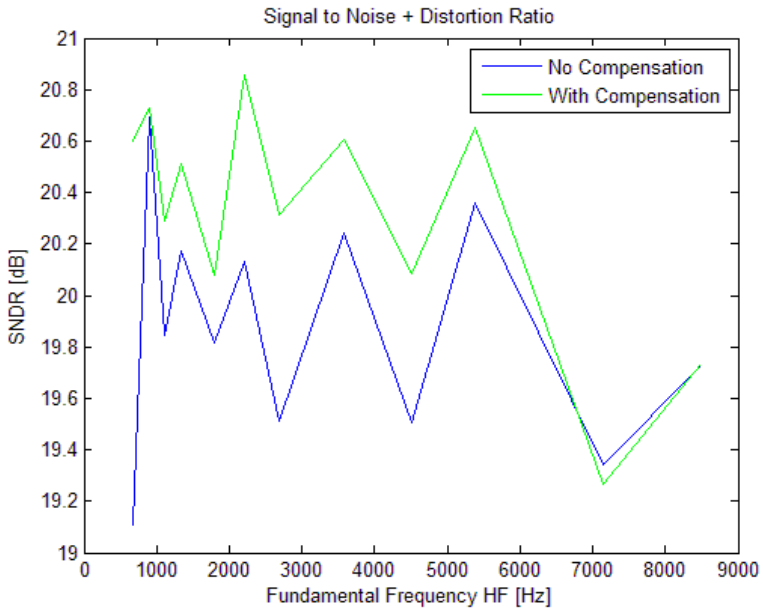

Figure 41: SNDR with and without compensation for the tone sequence

As shown in Figure 41, the SNDR is higher for all tones except the 11th and 12th at 7140 Hz and 8500 Hz. The mean dynamic range is 19.87 dB without compensation and 20.31 dB with compensation. For the 1st tone at 672 Hz, the increment in SNDR is 1.49 dB with compensation. For the 6th and 7th tone at 2210 Hz and 2682 Hz the increment in SNDR are 0.72 dB and 0.80 dB respectively.

To distinguish which of these distortion components that are audible, an equal loudness adjustment was done together with a masking evaluation. It was assumed that the sound pressure level at the woofer and tweeter were approximately at 80 dB_{SPL} and that the distortion components had an SPL around 30 dB. In Table 7, the result of the sideband component located at f_1-f_0 is presented where the equalizing value EQ is the adjustment of the distortion level in $dB_{SPL,}$ according to the equal loudness curve. The modulation distortion (M.D) columns are the equalized distortion levels relative the fundamental tone f_1. A masking threshold was approximated from both the tone at the woofer and tweeter, where the maximum level is included in the table. If the tone is not masked, the hearing threshold is given instead. The masking threshold was compared to the distortion level, resulting in an

evaluation if each distortion component is audible or not. Results for the components at f_1-f_0 are shown in Table 7.

Table 7: Resulting modulation distortion from second order components f_1-f_0

f_1 [Hz]	f_1-f_0 [Hz]	EQ [dB]	M.D No Comp [dB]	M.D Comp [dB]	Masking Threshold [dB]	Audible No Comp	Audible Comp
672	-	-	-	-	-	-	-
893	103	-26.4	-77.4	-77.1	-50	no	no
1105	315	-7.5	-61.9	-63.7	-65	**yes**	**yes**
1343	553	0.7	-53.8	-54.6	-55	**yes**	**yes**
1785	995	2.6	-54.7	-55.7	-35	no	no
2210	1420	-3.2	-63.1	-61.2	-35	no	no
2686	1896	-2.3	-61.2	-62.4	-40	no	no
3570	2780	2.0	-60.7	-58.7	-40	no	no
4505	3715	4.3	-51.8	-53.2	-35	no	no
5372	4582	5.3	-54.0	-54.2	-30	no	no
7140	6350	-15.2	-71.7	-69.8	-25	no	no
8500	7710	1.1	-56.6	-52.4	-20	no	no

In Table 7 it can be seen that only the distortion components located at 315 Hz and 553 Hz can be heard when the tones that give rise to them are present. The compensation damps these components by 1.8 dB_{SPL} and 0.8 dB_{SPL} for the 315 Hz and 553 Hz component respectively. An untrained listener can hear sound pressure differences of approximately 1 $dB_{SPL,}$ but a trained listener can distinguish smaller differences [13]. This indicates that the damping of these components can be heard as long as there are no other frequency components present in their proximity which masks them. The result from the sideband components located at f_1+f_0 is presented in Table 8.

Table 8: Resulting modulation distortion from second order components f_1+f_0

f_1 [Hz]	f_1+f_0 [Hz]	EQ [dB]	M.D No Comp [dB]	M.D Comp [dB]	Masking Threshold [dB]	Audible No Comp	Audible Comp
672	1462	-2,3	-58,0	-58,8	-30	no	no
893	1682	-2	-60,1	-60,6	-30	no	no
1105	1895	1,2	-54,5	-56,4	-30	no	no
1343	2133	5,4	-51,6	-52,0	-30	no	no
1785	2575	6,8	-50,1	-51,2	-30	no	no
2210	3000	4	-50,4	-51,1	-30	no	no
2686	3476	2,2	-53,8	-54,6	-30	no	no
3570	4360	0,4	-56,3	-56,7	-25	no	no
4505	5295	-0,9	-53,3	-57,3	-25	no	no
5372	6162	-1,7	-55,8	-57,1	-25	no	no
7140	7930	-21	-72,2	-70,6	-20	no	no
8500	9290	-2,1	-55,2	-54,1	-20	no	no

Table 8 shows that none of the generated distortion components are audible. This is because the masking is more evident in the frequency range above the maskee.

5.3 Listening test

The listening tests were performed in the sound lab at Lab.gruppen which is a small room of approximately $40\,m^3$. Two JBL SRX712M speakers were mounted on stands separated by 2 meters each with a tilt of 10°. A chair and table was placed 2 meters away from the middle point between the loudspeakers. Both loudspeakers were slanted so that they point towards the listener.

A Marantz CD4000/N3B CD player was connected through S/PDIF at 44.1 kHz/16 bit to a TC Electronic Finalizer for converting the S/PDIF signal to 96 kHz/24 bit. An external clock was used for the Finalizer generated by the MOTU 828mkII. The S/PDIF output from the Finalizer was connected to the MOTU 828mkII, which streams the signal through Firewire into AlgoFlex. A stereo implementation in AlgoFlex as described in Chapter 4 was used for the processing. The LF/HF outputs for the left and right channels were distributed through the analog outputs of the MOTU 828MkII to two separate PLM10000Q amplifiers. A neutral 2 channel coaxial module was used in the Lake Controller so that the amplifier solely amplified the signal. The LF/ HF outputs on each PLM10000Q were connected to a loudspeaker.

A GUI was implemented in MATLAB where the user could choose between A, B and X. These buttons control the gain of the compensation so that it is either on or off. Choice A was chosen to have no compensation, choice B had full compensation as had X. The user could also control the volume to a satisfying level and rewind or forward the music. A number of songs which were available to listen at are given in Table 9.

Table 9: Songs available for listening

Artist	Song
Björk	Hunter
Björk	Jóga
Björk	Unravel
Radiohead	Exit Music (For a Film)
Mark Kozelek	You ain't got a hold on me
Mark Kozelek	Find me, Reuben Olivares
Mark Kozelek	Around and Around
Red Hot Chili Peppers	Blood Sugar Sex Magik

A total of four people from Lab.gruppen listened to the music of choice and could choose freely from A, B and X. No one could distinguish if X was A or B. This indicates that the average listener will not be able to hear any difference with the compensation active on the JBL SRX712M either.

6 Discussion

If the transfer function from the voltage over the woofer to the current through the tweeter in Figure 17 is compared with the impedance of the tweeter in Figure 16, it can be seen that the

coupling is highest around the tweeters resonance peak. This is because the diaphragm of the tweeter moves more freely at this frequency. It also has its largest excursion at the resonance peak, which makes it probable that the source of frequency modulation distortion is dominant in this area.

The notch at 500 Hz of the transfer function in Figure 17 is probably caused by the modal properties of the baffle. If the estimated transfer function in Figure 17 is compared with the adaptive filter solution in Figure 26, it can be seen that the estimated frequency function has a higher amount of ripple. The ripple is probably a result of the high frequency resolution since not all frequencies are excited by the sweep.

The compensation damps the induced current from a maximum of 20 mA down to 2-5 mA. There are areas where the compensation does not reach full effect, which is at the lower frequencies and in the proximity of the notch. The discrepancies at the lower frequencies are caused by nonlinearities, which are dependent on the level of the voltage that is fed to the woofer. These nonlinearities seem to mainly affect the magnitude of the coupling. It is suspected that the notch has a slight deviation in frequency between different measurements, which causes less damping at nearby frequencies. An idea could be to remove it from the compensation filter since there is no use in defining something that doesn't exist.

Measurements have shown that the characteristics of the transfer function vary with where and how the loudspeaker is placed in the room. The impedance of a speaker is also temperature dependent, which implies that the static solution of the estimated transfer function in Chapter 3.3 is unfeasible in a real case scenario. Therefore, an adaptive solution has to be implemented, where the voltage of the woofer along with a low-pass filtered current from the tweeter are used as input signals. In the simulations an LMS algorithm was used because of the filter length, but other algorithms such as Fast Affine Projection could give a solution closer to the optimum, although it requires a verification of the stability [21].

Distortion measurements in the anechoic chamber show that the modulation distortion components mostly are reduced for fundamental frequencies up to 5372 Hz when the compensation is active, as described in Chapter 5.2. The components were not damped as much as suspected, although a damping of 30 dB of the induced current, which indicates that the remaining magnitude of the distortion components could be caused by the acoustical modulation distortion factors.

There were only two audible components at 315 Hz and 553 Hz when the resulting distortion was weighted with the equal loudness curve and compared to the masking levels. Their magnitude decreased with 0.8 dB_{SPL} and 1.8 $dB_{SPL,}$ which is an audible difference. This opts for that the improvement should be audible but it also requires that there are no other frequency components present in their proximity that masks them.

There is however a catch when it comes to the audibility of these distortion components. Since the masking is more evident in frequency regions above the masker, it could be assumed that the most audible distortion components are located at f_{HF}-f_{LF}. In most cases, the audible distortion will be present in the frequency band where the woofer is playing. Since it is the sound pressure of the woofer that generates the distortion components, it implies that the masking of the components increases with the level of the induced current, the source of

the distortion. It is simply a Catch 22 scenario. Therefore it is suspected that the results from the listening tests are caused by masking of distortion components appearing in this region and that the distortion from another speaker with higher coupling operating in a narrower frequency band could be audible.

An Adamson Y10 array loudspeaker was also measured in the anechoic chamber. The Y10 is a three-way system with two LF, two MF and one HF speaker. The coupling was higher for this loudspeaker but the results from distortion measurements showed that the modulation distortion increased, although the compensation was working well. It is likely that the current does not represent the motion of the speakers for the Y10. One could guess that it is likely that the speakers are not entirely de-coupled acoustically inside the box. An analysis of how the cone of the respective speakers behave with and without compensation using laser measurements could be done to examine this closer. A way to access the diaphragm has to be found in order to do these measurements, since it is not possible in the current design.

A question that naturally arises from the Y10 experience is if the diaphragm movement of the JBL SRX712M tweeter is totally compensated when the current is cancelled. Laser measurements for verifying the validity of the assumption that the induced current represents the diaphragm movement has to be done on another type of speaker than the JBL SRX712M. The hardware solution around the probes might be necessary to examine more closely as well to make sure that the measured current corresponds to the current through the tweeter.

It would be interesting to measure a coaxial speaker to get a better grip of the amount of modulation distortion generated by acoustical phenomena compared with that from an induced current. It might be also possible to get a clearer picture of what happens with the Adamson Y10 in such an analysis. A coaxial speaker is practically guaranteed to have a higher coupling between the bands implying that the modulation distortion will be higher for this type of speakers. Measurements done on the Adamson Y10 verifies that the coupling is significantly higher.

Other solutions for compensating the diaphragm displacement could be done acoustically and by electronic hardware. In the acoustical solution, a small pipe leading air could be inserted in between the cavity of the woofer and tweeter. The pressure generated by the woofer in front of the tweeter will then be compensated by the back side radiation of the woofer through the tube. An electronic hardware solution could be implemented by low-pass filtering the current at the tweeter and feed it back with an inverting amplifier.

7 Conclusions

It has been shown that there exists an acoustic coupling from the woofer to the tweeter on a two-way loudspeaker. Two different software solutions have been given that reduce the effect of this coupling with good results. Of the compensation methods, the adaptive filter solution turned out to be the best candidate, since it was discovered that the characteristics of the transfer function change with the speakers' placement. An LMS algorithm was chosen for the adaptive filter because of the extensively long impulse response.

Measurements of the distortion in an anechoic chamber prove that the coupling gives rise to modulation distortion and that the resulting components can be reduced by canceling the

induced current. An analysis on the audibility of the distortion was done by utilizing equal loudness and masking and it turned out that only 2 of a total of 24 components were supposed to be audible. Listening tests were done in an ABX fashion and none of the subjects could hear any difference between a non-compensated and a compensated system. It was assumed that the inaudibility of the distortion components was caused by masking from the woofer.

Furthermore, it is concluded that these results only are valid for the JBL SRX712M and that an audible difference is plausible when compensating another two-way or other type of loudspeaker.

8 Future Development

In order to get better measurements and to be able to measure and compensate the induced current at a lower sound pressure level, the signal to noise ratio of the current probe has to be increased. This is especially important if an adaptive filter is to be implemented in the DSP. An adaptive filter implementation also requires a design of a low-pass filter so that the algorithm can be run when the tweeter produces sound. A way to obtain a short latency from the filter has to be found, which for example could be done with the overlap-add method.

The LMS algorithm could be replaced by the Fast Affine Projection if a better convergence is desirable [22]. A lower magnitude limitation can be introduced for the adaptive filter so that the notch can be disregarded, leading to a better damping in the proximity of this frequency. A linearization can also be done to get a better damping at lower frequencies.

It would be really interesting to study other types of loudspeakers and see if any of these has audible distortion components. An analysis of how much of the modulation distortion that is caused by frequency modulation and amplitude modulation respectively could be performed. This would give a clearer idea of what types of speakers that should be studied further.

9 References

[1] P. Svensson, 'Electroacoustics & Ultrasonics; Useful formulae', *Department of Applied Acoustics*, Chalmers University of Technology, 1998.

[2] G. L. Beers and H. Belar, 'Frequency-Modulation Distortion in Loudspeakers', *J. Audio Eng. Soc., Vol. 29*, No. 5, pp. 320-326, 1981. (Originally published in 1943)

[3] J.C. Pedro and N.B. Carvalho, 'Intermodulation Distortion in Microwave and Wireless Circuits', *Artech House, Incorporated*, pp.25-71, 2003.

[4] P.W. Klipsch, 'Modulation Distortion in Loudspeakers', *J. Audio Eng. Soc., Vol. 17,* No. 2, pp. 194-206, 1969.

[5] P.W. Klipsch, 'Modulation Distortion in Loudspeakers: Part II', *J. Audio Eng. Soc., Vol. 18,* No.1, pp. 29-33, 1970.

[6] J. Moir, 'Doppler Distortion in Loudspeakers', *Preprint from presentation at the 46th Audio Eng. Soc. Convention*, pp.1-10, 1973.

[7] R H. Small, 'Measurement of Loudspeaker Amplitude Modulation Distortion', *114th Audio Eng. Soc. Convention, Paper 5731,* pp. 1-8, 2003.

[8] R. J. Mihelich, 'The Effects of Voice-Coil Rest Position on Amplitude Modulation Distortion in Loudspeakers', *113th Audio Eng. Soc. Convention, Paper 5640,* pp.1-25, 2002.

[9] *http://www.jblpro.com/catalog/general/Product.aspx?PId=113&MId=3*. Accessed 2009-10-28

[10] *http://www.labgruppen.com/downloads/product/PLM_Series_Technical_Data_Sheet_TDS_PLM10000Q_V13.pdf*. Accessed 2009-10-28.

[11] *http://www.behringer.de/EN/Products/ECM8000.aspx*. Accessed 2009-10-28.

[12] *http://www.motu.com/products/motuaudio/828mkII*. Accessed 2009-10-28.

[13] M. Kleiner, 'Audio Technology & Acoustics', *Division of Applied Acoustics, Chalmers University of Technology*, 2008. P.W. Klipsch, 'A Note on Modulation Distortion: Coaxial and Spaced Tweeter – Woofer Loudspeaker Systems', *J. Audio Eng. Soc., Vol. 24,* No.3, pp. 186-187, 1976.

[14] E. Zwicker and H. Fastl, 'Psychoacoustics', *Springer Verlag,* Berlin, 1990.

[15] B. Mulgrew, P. Grant and J. Thompson, 'Digital Signal Processing', *Palgrave Macmillan*, 2003.

[16] S. Muller and P. Massarani, 'Transfer-Function Measurement with Sweeps', *J. Audio Eng. Soc., Vol. 49,* No.6, pp. 443-471, 2001.

[17] *http://www.ta.chalmers.se/intro.php?page=facility#Anechoic*. Accessed 2009-10-16.

[18] P.W. Klipsch, 'A Note on Modulation Distortion: Coaxial and Spaced Tweeter – Woofer Loudspeaker Systems', *J. Audio Eng. Soc., Vol. 24,* No.3, pp. 186-187, 1976

[19] H. Suzuki and S. Shibata, 'Amplitude and Frequency Modulation Distortion of a Loudspeaker', *Preprint from presentation at the 74th Audio Eng. Soc. Convention,* pp.1-18, 1983.

[20] *http://www.mackie.com/products/tracktion3/*. Accessed 2009-12-03.

[21] M.J. Reed and M.O.J. Hawksford, 'Acoustic Echo Cancellation With the Fast Affine Projection', *Audio and Music Technology: The Challenge of Creative DSP (Ref. No. 1998/470), IEE Colloquium on 18 Nov. 1998,* pp. 16/1-16/8.

10 Appendix A: Challenges

A number of challenges occurred during this thesis work which will be given account for in this appendix.

In order to get things to work properly with Dante, the proper version supporting ASIO has to be installed; otherwise the synchronization with the PLM will not work. Dante Virtual Soundcard 1.0.0 for Windows was used which is the first version with the Dante Controller integrated. Running Dante and the MOTU 828mkII Firewire at the same time gives rise to glitches.

Problems with glitches also occur if Dante is used as a soundcard in AlgoFlex.

The full-scale reference levels were not documented for the Dante transmission of the probes so these had to be measured. The first recordings from the probes were done with Audacity 1.3 Beta. It turned out that even though the bit resolution is set at 24, the files were saved with a 16 bit resolution but with a header claiming 24 bits. This caused the measurements to be very noisy and almost impossible to use, since the recorded signal was far below the full-scale level. The only way this discrepancy could be verified was to measure the LSB and calculate what quantization level it corresponded to.

Tracktion has a master volume control which has a default gain of -3 dB. If a channel is panned all the way to the left or to the right, so that the sound is played in only one channel, it will have an extra gain of 6 dB. It also has an automatic playback of the recorded sound if that channel isn't muted with a gain of minus infinity. The automatic playback can be disabled by unselecting "enable end-to-end" in the Wave Audio Input settings.

The AutoGUI in AlgoFlex will not work with a sample rate of 96 kHz since the process cannot be started. This was only tested with version 1.0.6 and not with version 1.0.9. The routing for the MOTU soundcard is shifted with 2 steps e.g. selecting "Mains Out 1/2" gives outputs at "Analog Out 1/2".

If the amplifier gain for two 2aux channels was changed from 35 dB to 32 dB for module A and B in Lake Controller v5.1 and the power amplifier was restarted, the amplifier gain of module B changed itself back to 35 dB. It is unknown if this bug is present in the latest version.

It was hard to get good measurements at low levels because of the noise at the probes. The noise at the current probe had a level of approximately 2 mA_{pk}. This made the verification of the filters at a listening level impossible. When a PLM10000Q was used an entire day for measurements, the noise level for the current probe increased, which could be caused by heat. This is unwanted if an adaptive filter is going to be used.